Robustness of Gridded Precipitation Products for Vietnam basins using the Comprehensive Assessment Framework of Rainfall

Thanh–Nhan–Duc Tran [a,*], Manh–Hung Le [b,c], Runze Zhang [a], Binh Quang Nguyen [d], John D. Bolten [b], Venkataraman Lakshmi [a]

[a] Department of Engineering Systems and Environment, University of Virginia, Charlottesville, VA 22904, USA

[b] Hydrological Sciences Laboratory, NASA Goddard Space Flight Center, Greenbelt, MD 20771, USA

[c] Science Applications International Corporation, Greenbelt, MD 20771, USA

[d] Faculty of Water Resources Engineering, The University of Da Nang – University of Science and Technology, Da Nang 550000, Vietnam

*Corresponding author: Thanh–Nhan–Duc Tran (syu3cs@virginia.edu)

Abstract: The use of satellite–based precipitation products (SPPs) have become increasingly prevalent as key inputs to provide regional rainfall for improving hydrological simulations in data–spare regions. This study introduces a new approach – Comprehensive Assessment Framework of Rainfall (CAFR) to evaluate six satellite–based precipitation products (SPPs) for eleven basins with different sizes across Vietnam (2007 – 2015). These SPPs include the Global Precipitation Mission (GPM) Integrated Multi-satellitE Retrievals for Global Precipitation Measurement Final run Version 6 (GPM IMERGF V6), Multi–Source Weighted–Ensemble Precipitation (MSWEP) V2.2, Soil Moisture to Rain (SM2RAIN) – Advanced SCATterometer (ASCAT) V1.5, Asian Precipitation–Highly–Resolved Observational Data Integration Towards Evaluation (APHRODITE) V1901, Climate Hazards group Infrared Precipitation with Stations (CHIRPS) V2.0, and Precipitation Estimation from Remotely Sensed Information using Artificial Neural Networks (PERSIANN) – Climate Data Record (CDR) V1.0. With the proposed CAFR: (1) IMERGF is suggested to have the best performance overall, especially when simulating flood peaks; (2) SM2RAIN–ASCAT demonstrates the best skills in metrics related to the dry season; (3) For streamflow simulations, SPPs' performance is sensitive to basin size, with larger basins showing better performance skills. In this study, we demonstrate the capability of our proposed framework to better understand SPP applications in hydrological modeling.

Keywords: Comprehensive Assessment Framework of Rainfall (CAFR); Satellite–based precipitation products (SPPs); GPM IMERG; SM2RAIN; MSWEP; APHRODITE; CHIRPS; PERSIANN; Vietnam.

1. Introduction

Precipitation is the most important variable in quantifying the distribution of water budget inputs (Du et al., 2022; Nguyen et al., 2022a, 2023) and the water cycle rates across the globe (Beck et al., 2020; Chang et al., 2023; Ji et al., 2020; Sunilkumar et al., 2019; Tang et al., 2019; Thanh et al., 2022). It has been shown that accurate precipitation quantifications can substantially improve streamflow simulations, facilitating water management at both regional and global scales (Anjum et al., 2022; Mondal et al., 2018; Ren et al., 2018; Yuan et al., 2018; Libertino et al., 2016; Hashemi et al., 2017; Le et al., 2018; Dandridge et al., 2019; Fayne et al., 2017). However, measuring precipitation accurately is challenging due to various factors, such as its high variability in time and space, wind, and snow (Michaelides et al., 2009; Tapiador et al., 2012).

Rain gauges (RGs) are commonly recognized as the most reliable source for accurate rainfall data at a point scale (Derin & Yilmaz, 2014), but they are mostly centralized over the developed regions, limiting the availability of water inputs for hydrological simulations across a wide spatial coverage (Gerlak et al., 2011; Günter et al., 2013; McIntyre et al., 2005; Mondal et al., 2018; Plengsaeng et al., 2014). To overcome this challenge, researchers have used Satellite–based Precipitation Products (SPPs) that can provide the accumulated precipitation estimations over the ungauged and data–poor regions (Ji et al., 2020; Li et al., 2018; Ren et al., 2018). SPPs with a wider spatial extent, could provide rainfall data which is more accurate for use in hydrological models than data gathered directly from the ground.

The Asian Precipitation–Highly–Resolved Observational Data Integration Towards Evaluation (APHRODITE) product has been commonly used as a reference dataset in several regions, including Central Asia, Southeast Asia, and the Mekong River Basin (MRB) (Chen et al., 2017; Iqbal et al., 2022; Lauri et al., 2014). However, studies have shown that the APHRODITE tends to underestimate the annual rainfall by 13% – 25% and overestimate the number of extreme rainfall events (Ji et al., 2020; Lai et al., 2020; Tong et al., 2014). The lower accuracy of APHRODITE compared to other SPPs (i.e., Tropical Rainfall Measuring Mission (TPMM), Global Precipitation Climatology Centre (GPCC)) in terms of streamflow simulation and flood peak prediction has been mentioned in regional studies in Vietnam (Nguyen–Xuan et al., 2016; Nhi et al., 2019). The Multi–Source Weighted–Ensemble Precipitation (MSWEP) product has been widely used in recent years (Beck et al., 2020; Mondal et al., 2018), but it tends to overestimate or underestimate rainfall in semi–arid regions (Alijanian et al., 2017; Xu et al., 2019). Soil Moisture to Rain – Advanced SCATterometer (SM2RAIN–ASCAT), a new rainfall estimate using soil moisture (SM) data and bottom–up approach (Brocca et al., 2019; Rahman et al., 2019), struggles to estimate rainfall in regions with complex terrain or dense vegetation, particularly during extreme events (Brocca et al., 2014, 2019). SM2RAIN–ASCAT has also been found to underestimate peak rainfall and the presence of spurious rainfall events due to high–frequency changes in SM (Brocca et al., 2014, 2019;

Paredes–Trejo et al., 2018, 2019). It shows a high correlation, low Relative Bias (RB), and a good ability to detect moderate rainfall events but has problems in humid regions during the spring (Brocca et al., 2019).

Given those, SPPs have been extensively applied for drought monitoring and streamflow simulations (Le et al., 2020; Tran et al., 2023a). However, understanding the accuracy of those commonly used SPPs remains difficult due to the absence of a standardized evaluation scheme. The available assessment results often rely on a small subset of evaluation metrics by comparing against the overlapped ground–based precipitation measurements, and the preference for a certain metric could induce a biased judgment on the performance of SPPs. Additionally, the quality of SPPs is often analyzed from two aspects: the deviations relative to rain gauge measurements and their performance in simulating streamflow. For example, Le et al. (2020) assessed and compared eight gauge–corrected and gauge–uncorrected SPPs over six river basins in Vietnam in a combined use of comparison with rain gauges and evaluation of the SPP–driven simulations. Though comprehensive, the different validation results might generate diverged conclusions and thus distract decision–makers in determining the overall best SPPs candidate. Although an SPP is expected to exhibit comparable performances in precipitation estimation and streamflow simulations, which has been partially supported by the frequently great performance of rain gauge–driven simulations, it is not uncommon for the contrasted performances of an SPP in precipitation estimations and streamflow simulations over many areas. Thus, a rigorous evaluation framework that can coordinate multiple key metrics simultaneously and incorporates the bi–dimensional (i.e., precipitation estimation and streamflow simulation) performance is pressingly demanded.

This study introduces a Comprehensive Assessment Framework of Rainfall (CAFR) that accommodates all the above objectives. Our established framework combined different statistical metrics and the Multi–Criteria Decision Method (MCDM) to evaluate better and rank SPPs. Eleven basins have been chosen along with six different SPPs, including Integrated Multi-satellitE Retrievals for Global Precipitation Measurement (GPM IMERG) (Hou et al., 2014), MSWEP (Beck et al., 2019b), Climate Hazards group Infrared Precipitation with Stations (CHIRPS) (Funk et al., 2015), Precipitation Estimation from Remotely Sensed Information using Artificial Neural Networks – Climate Data Record (PERSIANN–CDR) (Ashouri et al., 2015), APHRODITE (Yatagai et al., 2012), and SM2RAIN–ASCAT (Brocca et al., 2019). This work shows a promising approach to assess SPPs, reveals the not–yet–evaluated products: MSWEP, SM2RAIN–ASCAT, as well as re–assess the APHRODITE product for Vietnam over different regions' characteristics (i.e., watershed's size, climate, terrain complexity, etc.). This research is important as it strengthens the accuracy and reliability of using SPPs in different regional conditions. By revealing the advantages and disadvantages of chosen products throughout assessments and the hydrological model

Soil and Water Assessment Tool (SWAT), this study contributes to developing and improving SPPs, fostering more accuracy of water resource estimation.

2. Watersheds

Eleven hydrological reference basins, as the finding from Do et al. (2022), have been chosen with basin areas between 383 km^2 and 6430 km^2 (Fig. 1) and average elevations ranging from 3 m to 2000 m (above mean sea level). These basins provide good spatial coverage and can serve as a foundation for any large–sample water resource study in Vietnam. They are the results of a systematic effort to identify a network of stations unaffected by ground anthropogenic activities. Each chosen basin area located in each sub–climatic region of Vietnam to known as North West (S1), North East (S2), North Delta (S3), North Central (S4), South Central (S5), Central Highland (S6), and South East (S7). These climatic regions have been defined based on their durations of rainy seasons, the three months with the heaviest rainfall, temperature, and differences in solar radiation (Nguyen & Nguyen, 2004).

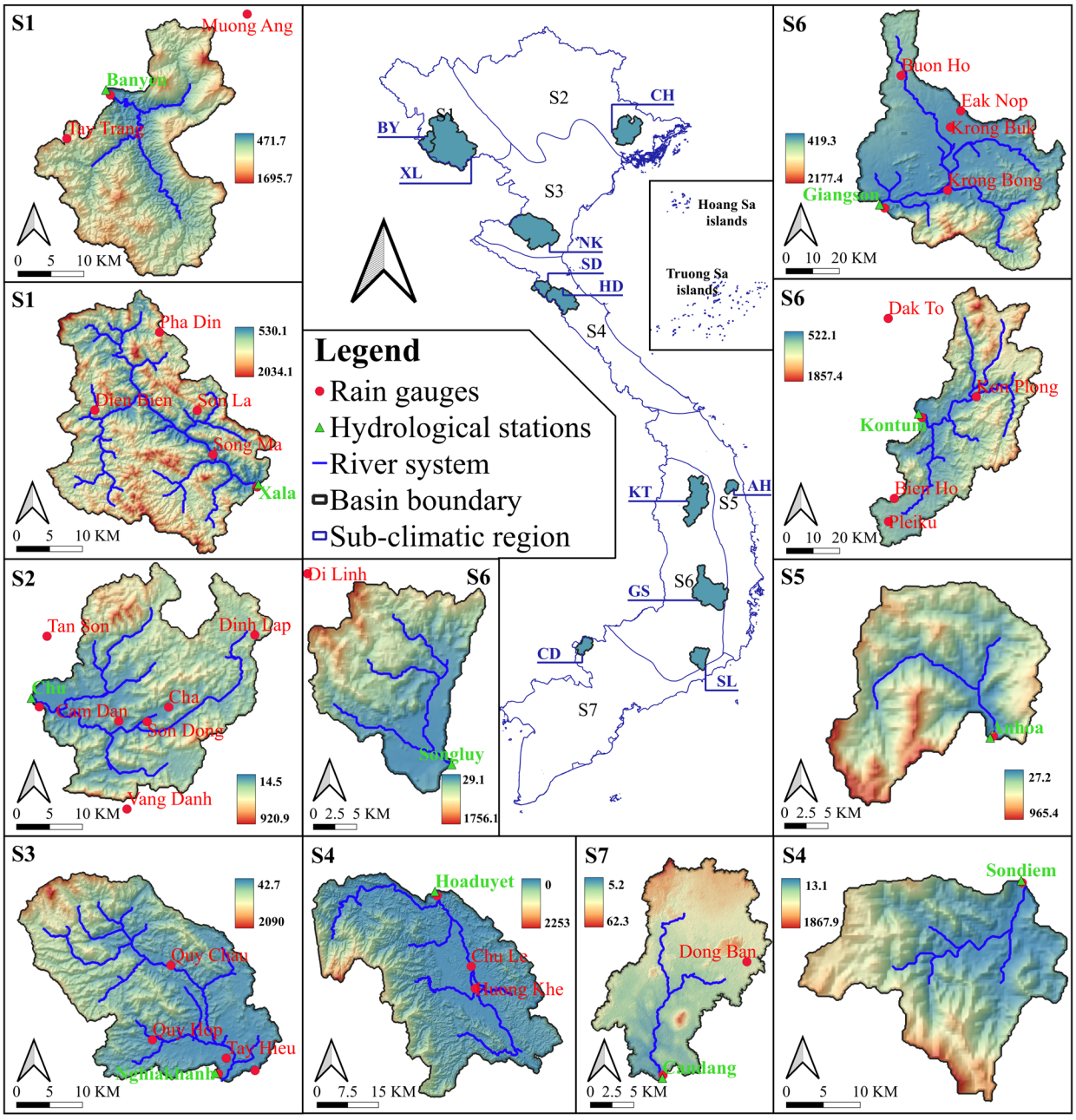

Fig. 1. Distribution of eleven basins across Vietnam with different climate characteristics and their meteorological stations. Legend in subpanels is Digital Elevation Model (DEM), with its units in meters.

3. Data and methods

The CAFR consists of three parts: (1) comparison of SPPs' characteristics, (2) hydrological simulations for streamflow simulation, driven by rain gauge and SPP, and (3) MCDM for ranking SPPs.

3.1. CAFR framework for evaluating SPPs

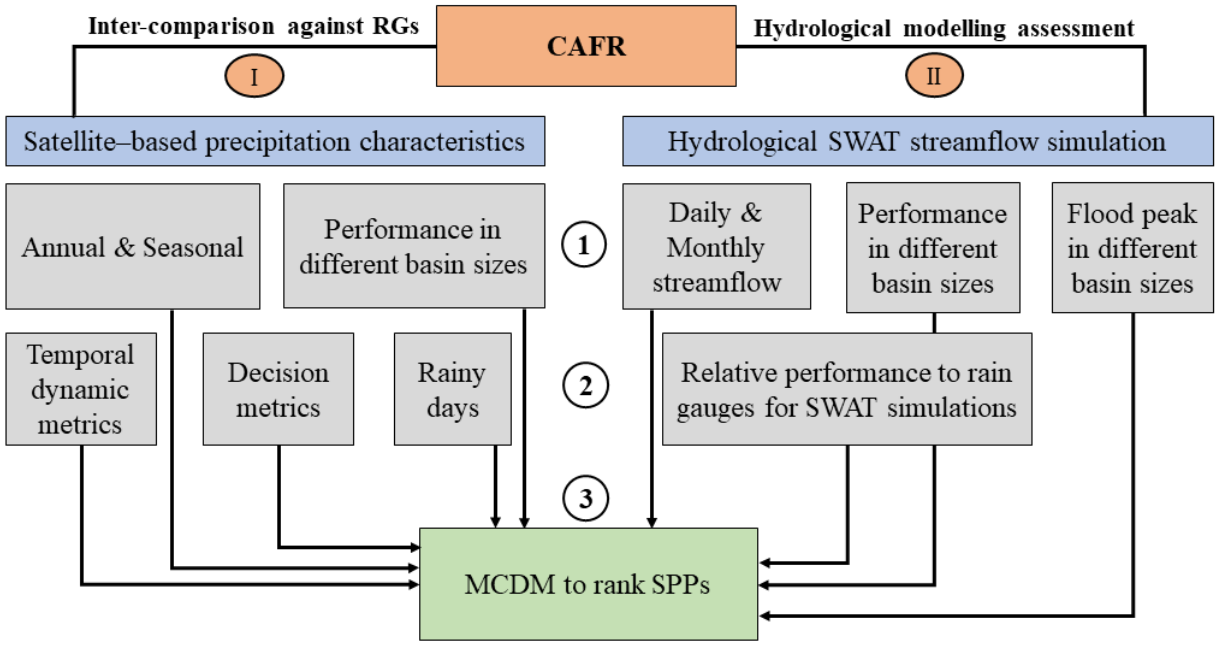

Fig. 2. The flowchart represents the sequential order of assessment stages of CAFR. The numerical values in the central nodes of the flowchart represent the order in which these stages were performed.

In (1), CAFR primarily analyzes the annual and seasonal performance of SPPs for rainfall estimation. It is important to understand seasonal rainfall patterns across different climatic regions and basin size levels. Besides, we also evaluate the streamflow simulation driven by rain gauges and SPPs. This evaluation is performed in similar terms of assessment (i.e., daily, monthly scales, and flood peak) for different basin sizes. This assessment aims to underline the correlation and consistency between results derived from inter-comparison and hydrological applications. These evaluations become important as they illustrate: the specific characteristics of SPPs in different basins' characteristics, and the strengths and weaknesses of SPPs in hydrological simulations.

An in–depth assessment of SPPs' performance is further described in (2), in which we employed statistical metrics (including temporal dynamic and decision metrics) and rainy–day detection. This is essential for assessing the performance of SPPs, and it offers significant support to drought detection studies (Fig. 2). Lastly, we calculate the correlation between the elevation range and rain gauge density using the formula $P_{relative} = (NSE_{SPP} - NSE_{RG})/NSE_{RG} \times 100$. This calculation helps illustrate the relative performance difference between SPPs and traditional rain gauges, thereby providing a comprehensive understanding of SPPs' effectiveness in different hydrological contexts.

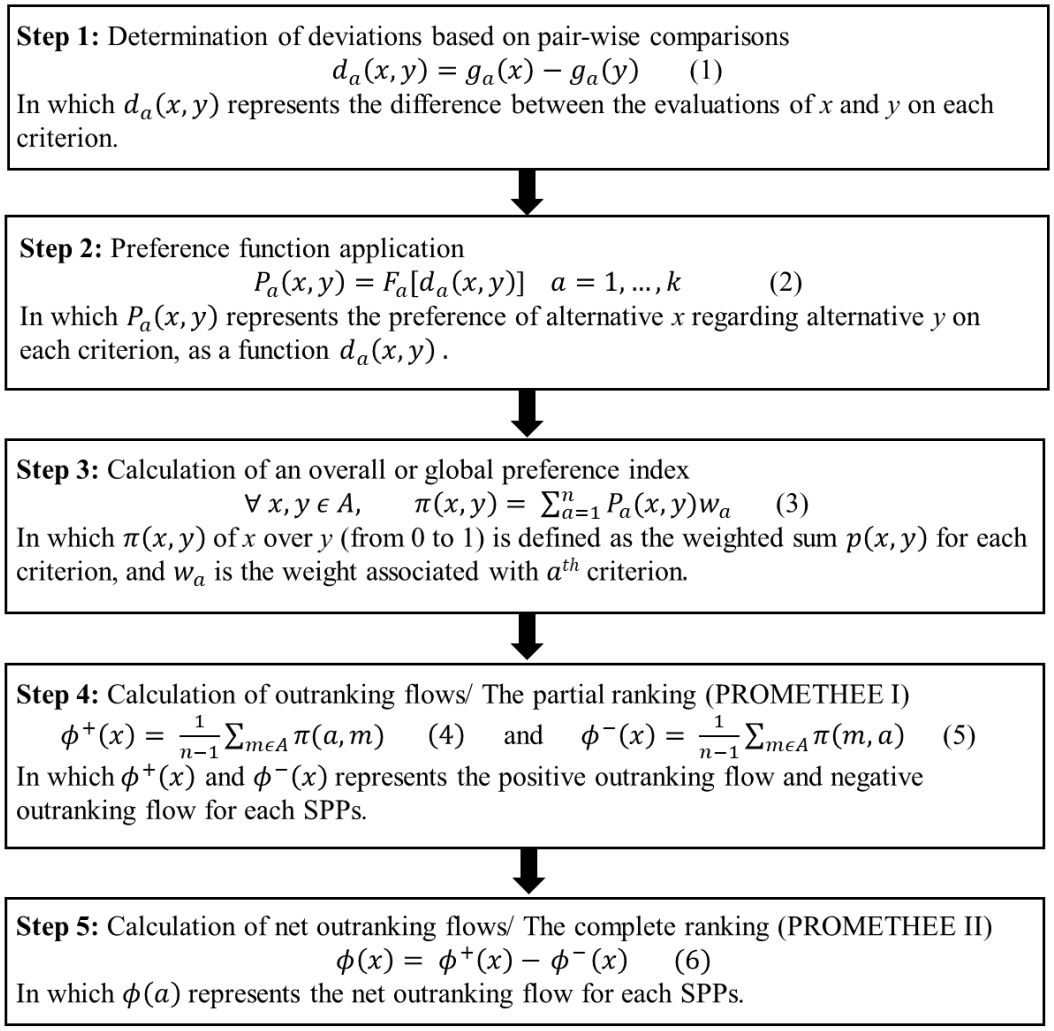

Fig. 3. MCDM method used in CAFR.

The MCDM used the Preference Ranking Organization Method for Enrichment Evaluations (PROMETHEE) family method (Behzadian et al., 2010) that was performed to obtain an accurate ranking of SPPs using results from (1) and (2) (Fig. 2). In our study, we utilized both the partial ranking of alternatives (PROMETHEE I) and complete ranking of alternatives (PROMETHEE II), as introduced by Brans et al. (1986). This dual–ranking approach allows us to score a finite number of alternatives while considering a variety of criteria. The PROMETHEE method sets itself apart from other MCDM methods through its unique internal process during decision-making, offering three key benefits: a user-friendly outranking approach, adaptability to real-life planning problems, and providing a complete ranking (Brans et al., 1986). The process we follow involves five main steps (Fig. 3):

- Conduct pairwise comparisons to identify disparities,
- Apply an appropriate preference function to each criterion,

- Calculate a global preference index,
- Determine both positive and negative outranking flows for each alternative and conduct a partial ranking,
- Calculate the net outranking flow for each alternative, resulting in the final ranking of SPPs.

3.2. In–situ data

Hydro–meteorological data were obtained from the Vietnam Meteorological and Hydrological Administration (VMHA) (http://kttvqg.gov.vn/). Prior to their use in this study, the data were collected and pre–processed by the hydrological services and regional meteorological authorities, ensuring their quality and reliability. The monthly observed runoff and rainfall for each basin are presented below, corresponding to the following regions: S1 (North West, XL, and BY basins of Ma River); S2 (North East, CH basin of Luc Nam River); S3 (North Delta, NK basin of Hieu River); S4 (North Central, HD and SD basins of Ngan Sau River and Ngan Pho Rivers, respectively); S5 (South Central, AH basin of Tra Khuc River); S6 (Central Highland, GS, KT basin and SL basins of Krong Ana, Dakbla, and Luy Rivers, respectively); and S7 (South East, CD basin of Sai Gon River).

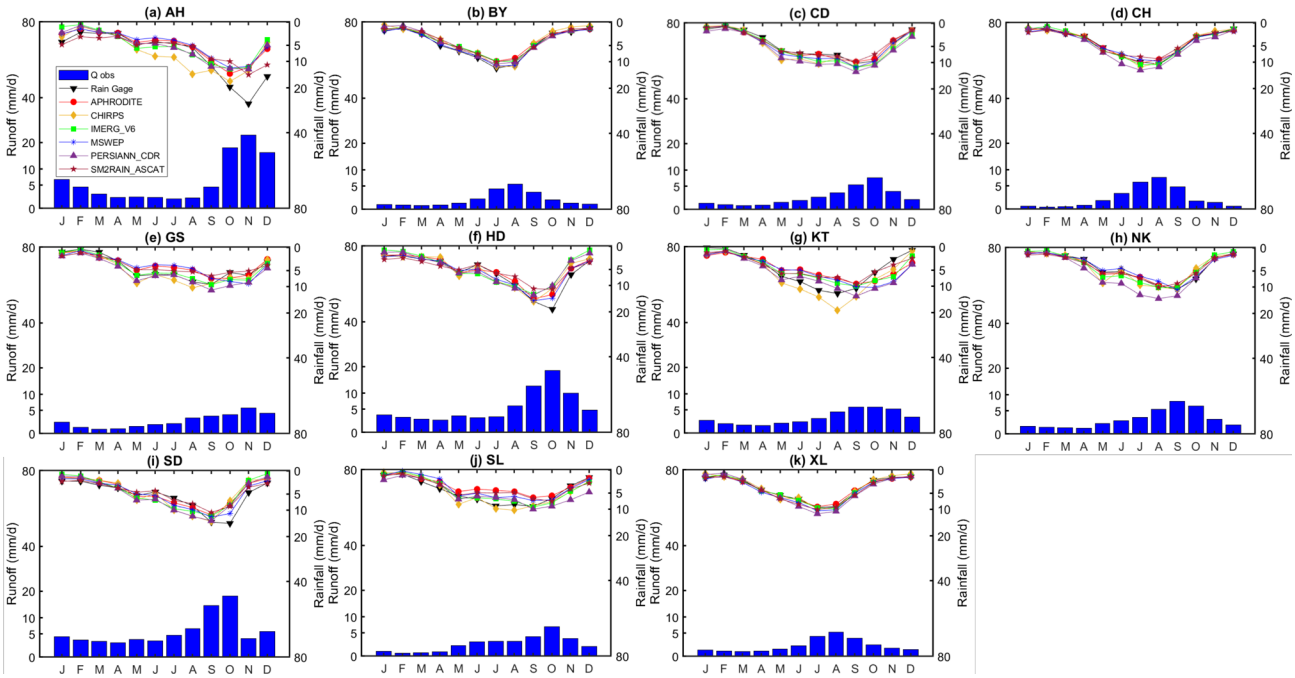

Fig. 4. The comparison between the observed monthly average runoff and monthly rainfall at basins' outlets: a) AH, b) BY, c) CD, d) CH, e) GS, f) HD, g) KT, h) NK, i) SD, g) SL, and k) XL basins.

The daily rainfall data was obtained from the 39 rain gauge stations for the chosen eleven basins, while the daily runoff data at basins' outlets were obtained for the same simulation period (2007 – 2015). The

169 average percentage of missing values over all rain gauges was less than 1.0%. For small–size basins such
170 as AH (383km^2), SD (599km^2), CD (617km^2), and BY (638km^2), the number of rainfall stations used would
171 vary from one to three, while other basins (with area higher than 700km^2) would have from three to six
172 rainfall stations. The locations of eleven basins of Vietnam are shown in Figure 1, in which the peak
173 monthly runoff varies from August (BY and XL basins – zone S1 and CH basin – zone S2) to September
174 (KT basin – zone S6 and NK basin – zone S3), October (CD basin – zone S7, HD, and SD basins – zone
175 S4, and SL basin – zone S6), and November (AH basin – zone S5, and GS basin – zone S6). The largest
176 runoff among basins was found in November at AH basin (Fig. 4). Additionally, the minimum and
177 maximum temperatures of the air were obtained at meteorological stations, and the length of these datasets
178 has been maintained the same compared to precipitation datasets measured from rain gauges.

179 *3.3. Description of SPPs*

180 *3.3.1. IMERG*

181 IMERG product is a type 3 level dataset that employs the GPM estimation algorithm and endeavors to
182 integrate, interpolate, and intercalibrate several estimates of microwave precipitation obtained from satellite
183 sources (Hou et al., 2014; Yuan et al., 2018). In this study, the 0.1° gridded IMERGF (V6.0) was used, and
184 it can be obtained from (https://pmm.nasa.gov/data–access/downloads/gpm).

185 *3.3.2. MSWEP*

186 MSWEP product is a recent global rainfall dataset that captures rainfall on a 3–hourly temporal scale.
187 It was developed by Beck et al. (2019b) and draws on the strengths of reanalysis–based, gauge–based, and
188 satellite–based datasets to generate precise estimates of precipitation worldwide. The 0.1° gridded MSWEP
189 (V2.2) dataset was used and can be obtained from (http://www.gloh2o.org/mswep/).

190 *3.3.3. SM2RAIN–ASCAT*

191 SM2RAIN–ASCAT product is a recently developed global–scale rainfall dataset based on satellite SM
192 measurements obtained from the European Meteorological Satellite's Advanced SCATterometer.
193 SM2RAIN algorithm is used as the bottom–up approach to compute precipitation changes using SM data,
194 as described in previous studies by Brocca et al. (2014, 2019) and Wagner et al. (2013). The 0.125° gridded
195 SM2RAIN–ASCAT (V1.5) dataset was used and can be obtained from
196 (https://zenodo.org/record/6136294).

197 *3.3.4. APHRODITE*

APHRODITE is a 0.25° long–term continental–scale, rain gauge network interpolated precipitation product (Yatagai et al., 2012). To construct APHRODITE, three rain–gauge datasets have been used: APHRODITE own collection rain gauge network; Global Telecommunication System data; and other projects' datasets (Ji et al., 2020; Yatagai et al., 2012). The 0.25° gridded APHRODITE (V1901) dataset was used and can be obtained from (https://www.chikyu.ac.jp/precip/).

3.3.5. CHIRPS

CHIRPS is a product of the Climate Hazards Group at the University of California–Santa Barbara, designed to detect droughts to aid the United States Agency for International Development Famine Early Warning System Network, as explained by Shen et al. (2020). The 0.05° gridded CHIRPS (V2.0) was used and can be obtained from (https://www.chc.ucsb.edu/data/chirps).

3.3.6. PERSIANN–CDR

The PERSIANN–CDR is a satellite precipitation product that is mostly based on the brightness temperature of infrared images made by geostationary satellites in combination with the Climate Data Record (CDR) (Ashouri et al., 2015; Hsu et al., 1997; Tan & Santo, 2018). The 0.25° grided PERSIANN–CDR (V1.0) was used and can be obtained from (https://chrsdata.eng.uci.edu/).

Table 1 Descriptions of used SPPs for this study.

SPP	Temporal coverage	Resolution	Spatial coverage	Temporal resolution	Latency	References
IMERGF–V6	2000 – 2021	0.1°	65°N – 65°S	1/2h	Several months	Hou et al., 2014
MSWEP V2.2	1979 – present	0.1°	60°N – 60°S	3h	Several days	Beck et al., 2019b
SM2RAIN–ASCAT V1.5	2007 – 2021	0.125°	60°N – 60°S (land)	Daily	N/A	Wagner et al., 2013
APHRODITE V1901	1951 – 2015	0.25°	60°N – 60°S	Daily	24 hours	Yatagai et al., 2012
CHIRPS V2.0	1981 – present	0.05°	50°N – 50°S	Daily	24 hours	Funk et al., 2015
PERSIANN–CDR V1.0	1983 – present	0.25°	60°N – 60°S	Daily	Several months	Ashouri et al., 2015

Table 2 Statistical metrics for evaluating SWAT and SPPs performance.

	Metric	Equation	Optimal value	Criterion
Inter–comparison with rain gauges Metrics	Probability of Detection (POD)	$\frac{D_{11}}{D_{11}+D_{01}}$	1	
	False Alarm Ratio (FAR)	$\frac{D_{10}}{D_{11}+D_{10}}$	0	
	Critical Success Index (CSI)	$\frac{D_{11}}{D_{11}+D_{01}+D_{10}}$	1	
	Correlation Coefficient (CC)	$\frac{\sum_{i=1}^{N}(RG_i-\overline{RG})(SPE_i-\overline{SPP})}{\sqrt{\sum_{i=1}^{N}(RG_i-\overline{RG})^2\sum_{i=1}^{N}(SPP_i-\overline{SPP})^2}}$	1	
	Relative Bias (RB)	$\frac{mean(SPP)}{mean(RG)}-1$	0	
	Root Mean Square Error (RMSE)	$\sqrt{\frac{1}{n}\sum_{i=1}^{N}(SPP_i-RG_i)^2}$	0	
Streamflow Performance Metrics	Nash–Sutcliffe Efficiency (NSE)	$1-\frac{\sum_{i=1}^{N}(obs_i-sim_i)^2}{\sum_{i=1}^{N}(obs_i-\overline{obs_i})^2}$	1	VG: $1 \geq NSE \geq 0.8$, G: $0.80 \geq NSE \geq 0.70$, S: $0.70 \geq NSE \geq 0.50$, NS: $NSE < 0.5$
	Percentage Bias (PBIAS)	$\left(\frac{\sum_{i=1}^{N}(obs_i-sim_i)}{\sum_{i=1}^{N}obs_i}\right)\times 100$	0	VG: $PBIAS \geq \pm 5$, G: $5 \leq PBIAS \leq \pm 10$, S: $\pm 10 \leq PBIAS \leq \pm 15$, NS: $PBIAS > \pm 15$

Note: D_{11} is the precipitation measured by the rain gauge and the satellite simultaneously. D_{10} represents the precipitation detected by the satellite but not by the rain gauge. D_{01} is the opposite of D_{10}. $\mathrm{sim_i}$ denotes the simulated streamflow while $\mathrm{obs_i}$ indicates the observed streamflow (m^3/s). The average simulated

streamflow is represented by $\overline{sim}$ while the average observed streamflow is denoted by $\overline{obs}$ (m^3/s). Very Good denotes VG, Good denotes G, Satisfactory denotes S, and Not Satisfactory denotes NS.

3.4. SWAT model

SWAT is a watershed–scale model that is semi–distributed and was developed and supported by the United States Department of Agriculture (USDA) and the Agriculture Research Service (ARS), as detailed by Arnold et al. (2012). This model has been used in many studies to address different hydrological–related problems, including land–use land cover, chemical pollution from pesticides and agricultural chemicals on streamflow and sediment loads, ecosystem management, and climate change (Mohammed et al., 2018a, 2018b, 2018c; Ashrafi et al., 2022a, 2022b; Behboudian et al., 2021; Le et al., 2020; Nguyen et al., 2022; Tran et al., 2023a, 2023b; Tapas et al., 2022a, 2022b). The SWAT model predicts runoff using DEM, land–use, and soil information, which are stored in Hydrologic Response Units (HRUs) (Arnold et al., 2012). Runoff is calculated separately for each HRU, and the total runoff for sub–basins and the entire basin is determined by adding the HRU runoffs (Arnold et al., 2012). The input requirements for the SWAT model are summarized in Table 3.

Table 3 Description of SWAT required inputs in this study.

Dataset	Description	Source
DEM	The 90–m DEM estimates the slope and delineates the basin boundary, validated using the Vietnam National Basin database reference with an average error of less than 3%.	HydroSHEDS Core layers (V1.0) (https://www.hydrosheds.org/products/hydrosheds)
Land–use land cover	A 30–m land–use land cover map was downloaded from SERVIR–Mekong website for 2010.	SERVIR–Mekong (https://www.landcovermapping.org/en/home/)
Soils data	A 30–m soil map with a scale of 1:1,000,000 resampled from polygons to raster format.	National Institute for Soils and Fertilizers. (2002)

Weather data	The daily precipitation, temperature, and rainy–day threshold (0.6 mm/day) were obtained from VMHA between 2007 and 2015. Six SPP datasets and rain gauges were utilized for streamflow simulation using the SWAT model, and seven simulation scenarios were conducted for each basin (2007 – 2015).	• Ground data: VMHA • SPPs: IMERGF–V6; MSWEP V2.2; SM2RAIN–ASCAT V1.5; APHRODITE V1901; CHIRPS V2.0; PERSIANN–CDR V1.0; (please see Table 1 for detailed description)

The basin delineation and HRUs creation was carried out using QSWAT (V1.5.2) in the QGIS (V3.16.19) platform (Dile et al., 2016), and the watershed was delineated using Terrain Analysis Using Digital Elevation Models (TauDEM) (V5.0) (Oals, 2011). In the SWAT model setup, a contributing area threshold of 25 km^2 and a filter threshold of 10% were used for slope, land use, and soil to ensure the presence of a minimum of 3 (CA, AH) to 51 (XL) sub–basins in this study.

Due to differences in dataset availability for SPP products (Table 1), we chose the overlapping period (2007 – 2015) for all SPPs to perform our analysis and hydrological simulation. The model was performed on a daily timescale, with two years warm–up period (2007 – 2008) and a simulation period (2009 – 2015). The calibration period was set from 2009 to 2012, while the validation was performed between 2013 and 2015.

The study used SWAT–CUP and the Sequential Uncertainty Fitting method V2 (SUFI–2) method for model calibration and validation, as the findings of Abbaspour et al. (2007, 2015). The calibration and validation involved 4,000 runs for each scenario to obtain the optimal fitted values. NSE was used as the objective function in the SWAT–CUP program. This study selected 23 parameters, with their names, methods, descriptions, ranges, and fitted values could be found in Supplementary Data S1.

3.5. Statistical performance metrics

Table 2 denotes the formulas and optimal scores for the statistical performance metrics. To compare SPPs with the rain gauges, the Probability of Detection (POD); False Alarm Ratio (FAR), and Critical Success Index (CSI) were used. For the temporal dynamic evaluation, Correlation Coefficient (CC), Relative Bias (RB), and Root Mean Square Error (RMSE) were used. For streamflow performance, Nash-Sutcliffe Efficiency (NSE) and Percentage Bias (PBIAS) (Moriasi et al., 2007, 2015) were used. The POD gives the proportion of real rainfall events that the SPP products can identify. FAR measures the fraction of false precipitation events from SPP products compared to total rainfall events. Based on POD and FAR, CSI is

the most balanced detection metric. CC measures the similarity between SPP products and ground observations. RB and RMSE quantify the bias and accuracy of satellite estimates. NSE measures the relative magnitude between the simulated and observed streamflow. The PBIAS quantifies the average inclination of the simulated streamflow to overestimate or underestimate the observed streamflow consistently.

4. Results and discussion

4.1. Inter–comparison of SPPs' characteristics and rain gauges

For the inter–comparison of SPPs, we assessed the characteristics of six SPPs using observations from rain gauges across eleven basins (Fig. 1). We matched precipitation values extracted from SPP's grids to the rain gauge locations. If more than one rain gauge was located in a grid, we averaged values from those gauges before the comparison.

4.1.1. Annual and seasonal rainfall distributions

Figure 5 represents the mean annual precipitation over Vietnam from (a) APHRODITE, (b) CHIRPS, (c) IMERGF, (d) MSWEP, (e) PERSIANN–CDR, and (f) SM2RAIN–ASCAT, respectively. The mean rainfall estimates have been calculated between 2007 and 2015 for all chosen SPPs. The wet and dry seasons for each climate region have been classified by Nguyen & Nguyen. (2004) (Fig. 5) (see Supplementary Data S2).

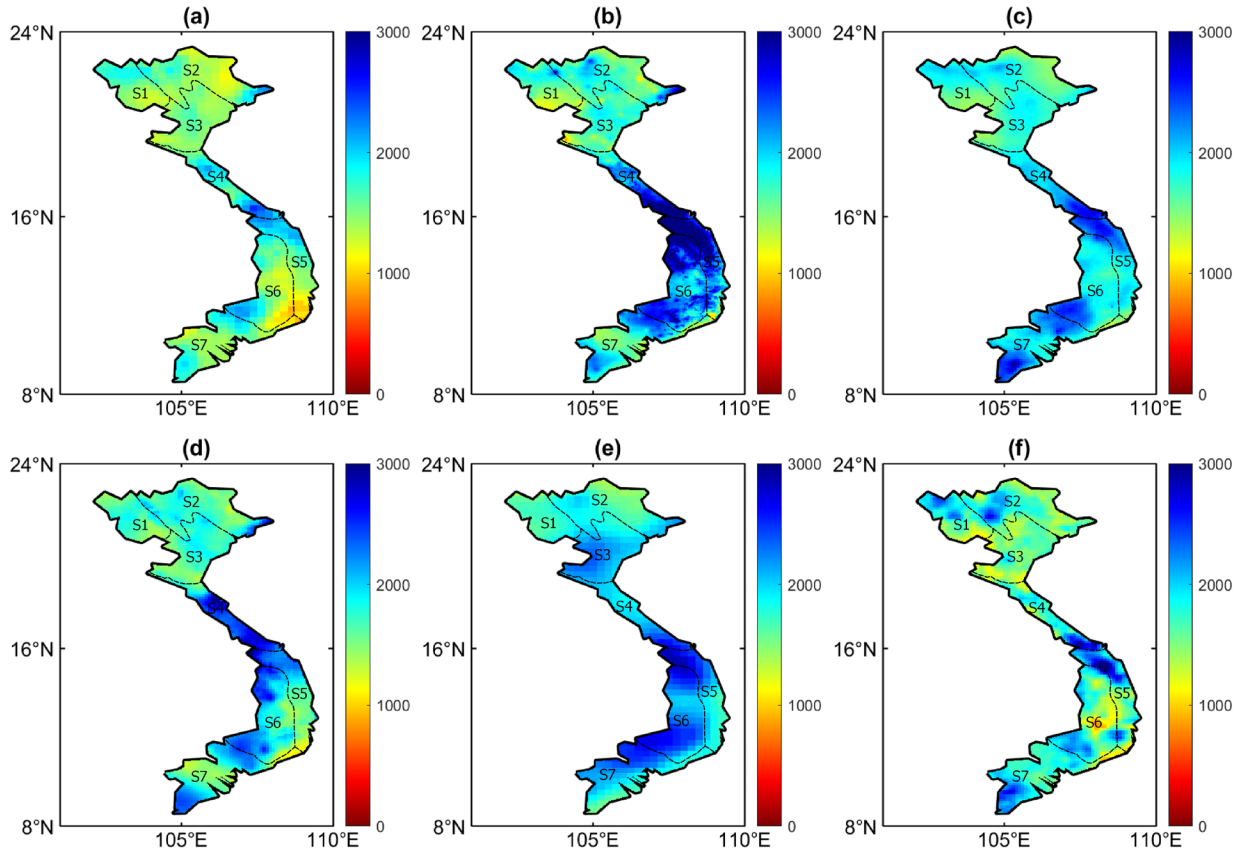

Fig. 5. Mean annual precipitation for Vietnam from a) APHRODITE, b) CHIRPS, c) IMERGF, d) MSWEP, e) PERSIANN–CDR, and f) SM2RAIN–ASCAT.

APHRODITE, CHIRPS, and SM2RAIN–ASCAT showed high differences in the S4, S5, and S6 regions. CHIRPS and PERSIANN–CDR captured more rainfall in S5 and S6 (Fig. 5), while APHRODITE showed less rainfall measured along the coast.

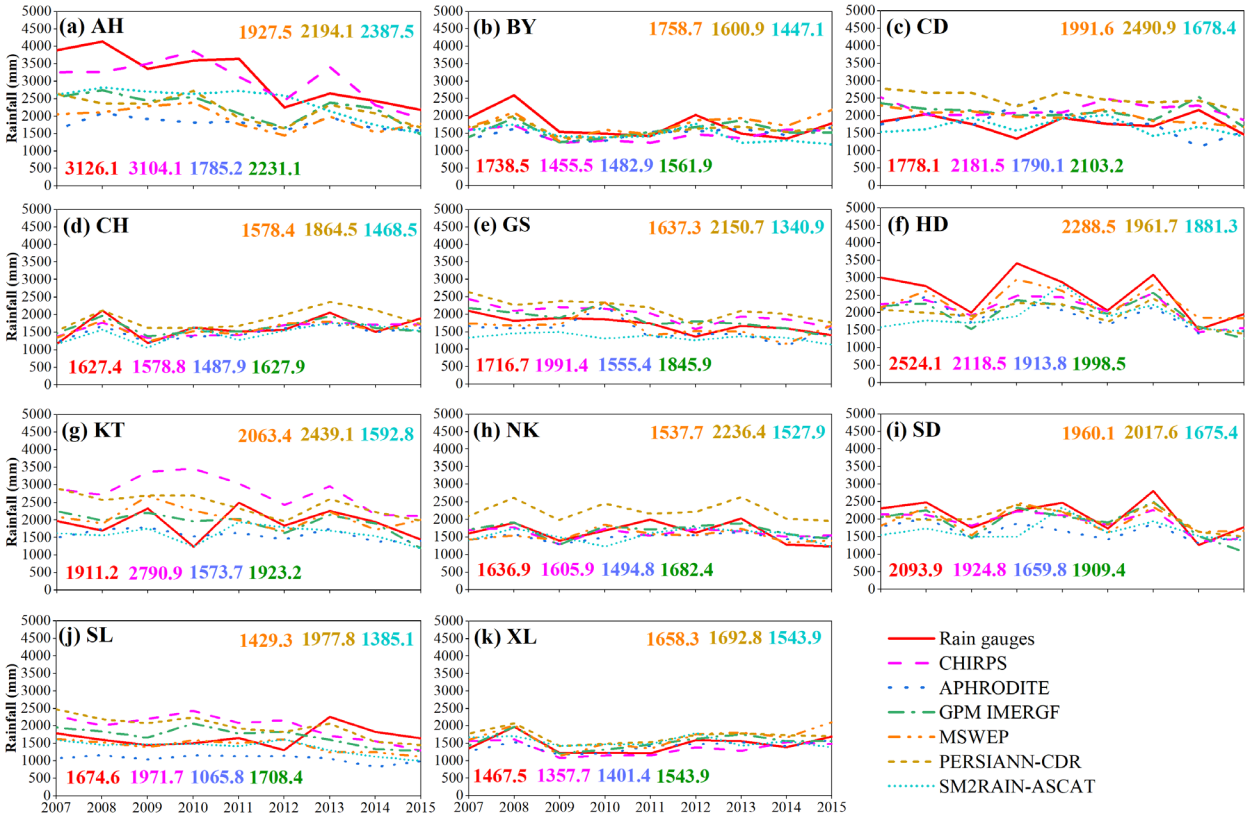

277

278 **Fig. 6.** Annual rainfall for a) AH, b) BY, c) CD, d) CH, e) GS, f) HD, g) KT, h) NK, i) SD, j) SL, and k)
279 XL. The mean value of rainfall estimates for each SPP is represented by a value in bold with corresponding
280 colors.

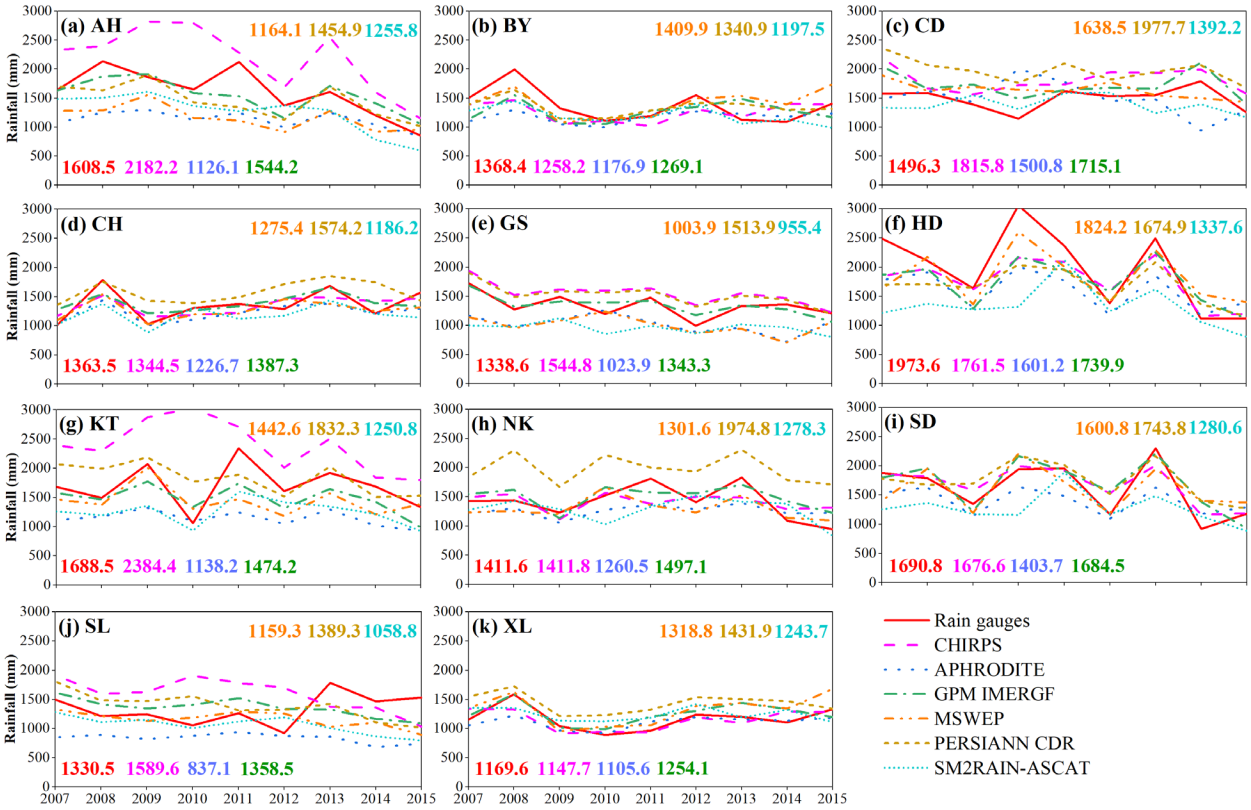

Fig. 7. Wet season rainfall for a) AH, b) BY, c) CD, d) CH, e) GS, f) HD, g) KT, h) NK, i) SD, j) SL, and k) XL. The mean value of rainfall estimates for each SPP is represented by a value in bold with corresponding colors.

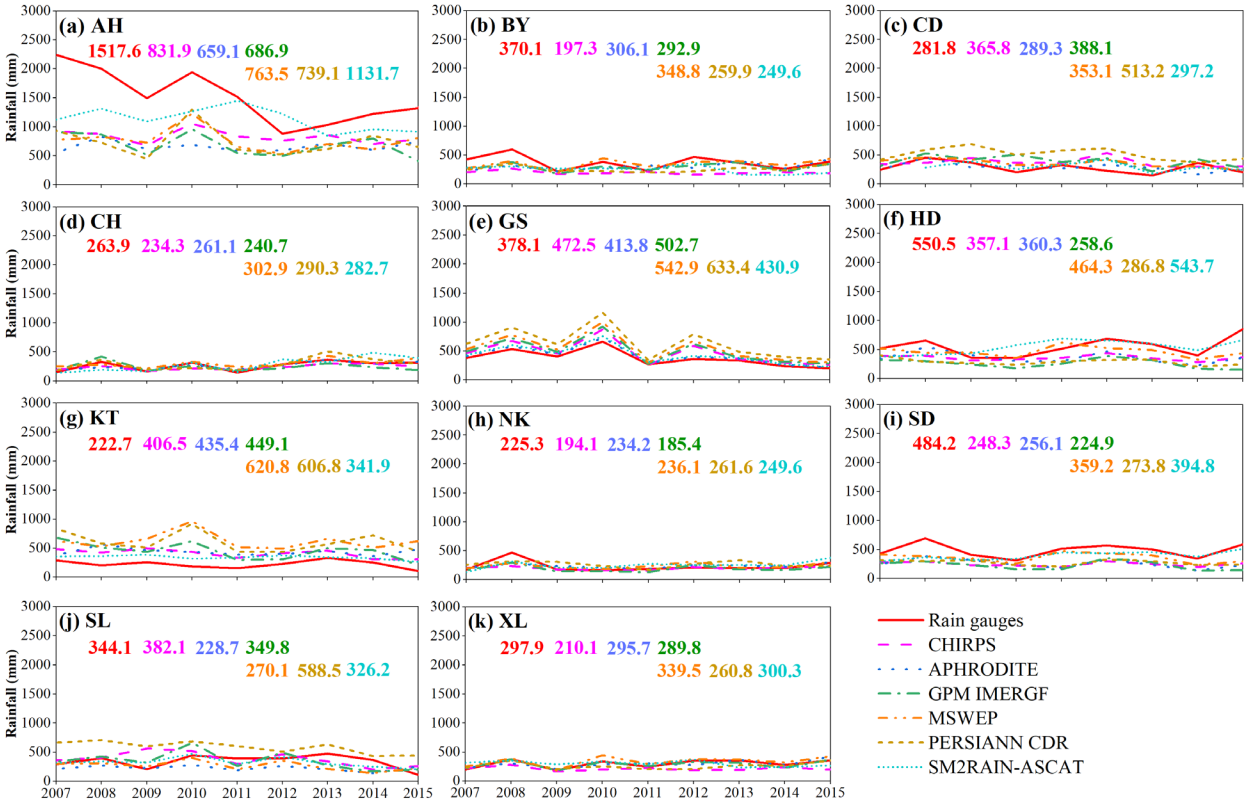

Fig. 8. Dry season rainfall for a) AH, b) BY, c) CD, d) CH, e) GS, f) HD, g) KT, h) NK, i) SD, j) SL, and k) XL. The mean value of rainfall estimates for each SPP is represented by a value in bold with corresponding colors.

We combined the assessment of SPPs' performances in different basin sizes (Table 4). We categorized different basin size levels with large (> 4000 km^2), medium (≤ 4,000 km^2 and > 1000 km^2), and small (≤ 1000 km^2) to compare SPPs and rain gauges.

Table 4. The difference (in percentage) of rainfall estimates between SPPs and rain gauges for different basins' area levels. Bold values indicated the best score.

Period	Basin size	IMERGF	MSWEP	SM2RAIN–ASCAT	APHRODITE	CHIRPS	PERSIANN–CDR
Annual	Large	**3.99**	9.53	5.93	6.60	4.69	25.98
	Medium	7.25	**6.23**	18.44	14.95	20.27	22.44
	Small	**13.58**	14.51	16.65	23.07	13.67	19.91
Dry	Large	10.21	9.37	5.80	**2.36**	21.68	14.30
	Medium	49.11	63.22	**18.98**	35.15	38.48	74.49
	Small	33.71	25.62	**17.42**	31.44	36.29	55.54

Wet	Large	6.64	10.28	7.89	8.09	**0.95**	31.16
	Medium	**6.66**	13.40	24.94	21.25	17.19	13.05
	Small	**6.52**	10.72	16.45	18.84	17.74	11.29

Most SPPs showed better rainfall estimation when the watershed size increased except PERSIANN–CDR, especially during the wet season (Table 4). IMERGF showed a high capability for annual rainfall estimates with the lowest difference of 0.63% (S6 region), 2.78% (S3), and highest (5.21%) in S2 (Fig. 6). MSWEP showed similarities compared to IMERGF in which the lowest difference (1.16%) was found in S1 region, and the highest (6.06%) is in S3 region. IMERGF showed a high similarity for the rainfall estimates over different basin sizes, highest in large basins and lower when the basin size decreases (Table 4).

MSWEP overestimated rainfall in coastal basins (S5) (28.63% difference) and in semi–arid region (S6) (14.65% difference), compared to rain gauges (Fig. 6). These estimations could be explained by the algorithm used for bias reduction as well as the non–uniformity in the spatial distribution of rain gauge data. CHIRPS and PERSIANN–CDR overestimated the annual rainfall in S7 by 22.69% and 40.09%, respectively, compared to rain gauges. Besides, CHIRPS overestimated the S6 region rainfall with the lowest difference of 16.00% to the highest of 46.03% (Fig. 6).

SM2RAIN–ASCAT underestimated the total precipitation over eleven basins during the wet season, which could be explained due to the high water content resulting in the saturation of the soil, as mentioned by Brocca et al. (2014) and Paredes–Trejo et al. (2019). In addition, SM2RAIN–ASCAT showed less capability to capture rainfall in basins with high variation of rainfall patterns (i.e., KT with 25.92% difference – S6; HD with 32.22% – S4) (Figs. 6 – 8). During the dry season, SM2RAIN–ASCAT performed the best over small, medium, and large–size basins (Table 4).

APHRODITE underestimated the seasonal and annual rainfall, especially in the coastal basin (S6) (Fig. 7). It showed good rainfall estimates in large basins with the lowest difference of 5.80% and became worse in medium and small basins, compared to rain gauges (Table 4). Additionally, APHRODITE showed a worse rainfall estimate during the dry season for S4 and became significantly less accurate in the semi–arid region, with the highest difference of 95.54% compared to rain gauges. This finding is consistent with the findings of Ahmed et al. (2019), in which APHRODITE showed the highest error for rainfall estimates over Pakistan. APRHODITE significantly underestimated/overestimated rainfall when the watersheds' areas decreased.

4.1.2. SPPs comparison using rainfall detection metrics and rainy–days detection

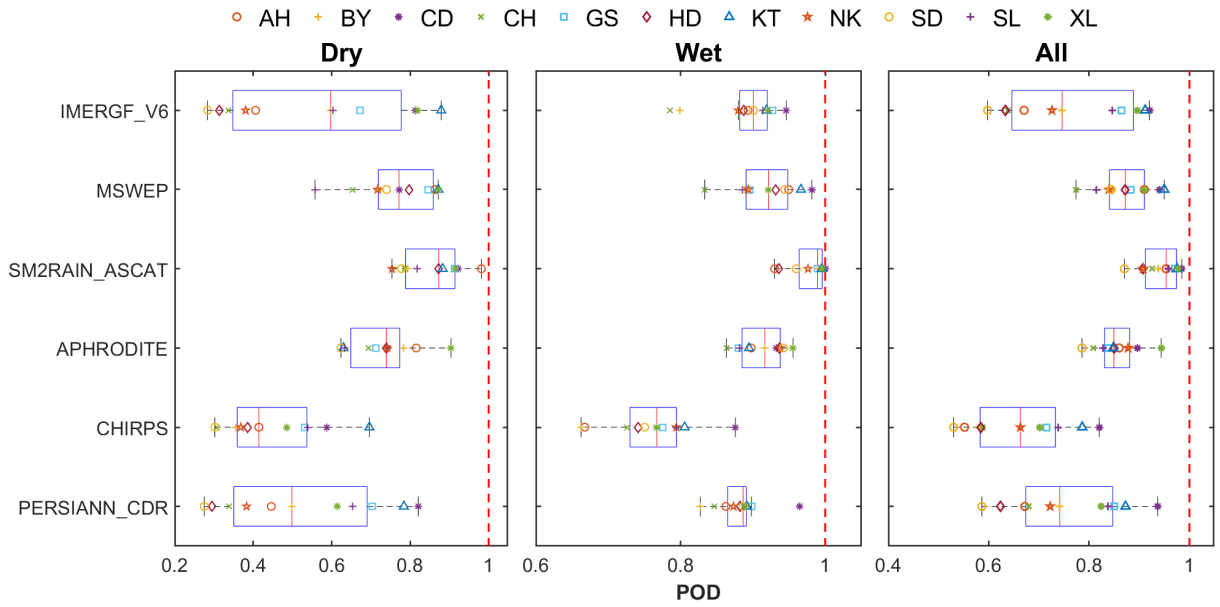
AH BY CD CH GS HD KT NK SD SL XL
Dry
Wet
All
IMERGF_V6
MSWEP
SM2RAIN_ASCAT
APHRODITE
CHIRPS
PERSIANN_CDR
0.2 0.4 0.6 0.8 1
0.6 0.8 1
0.4 0.6 0.8 1
POD

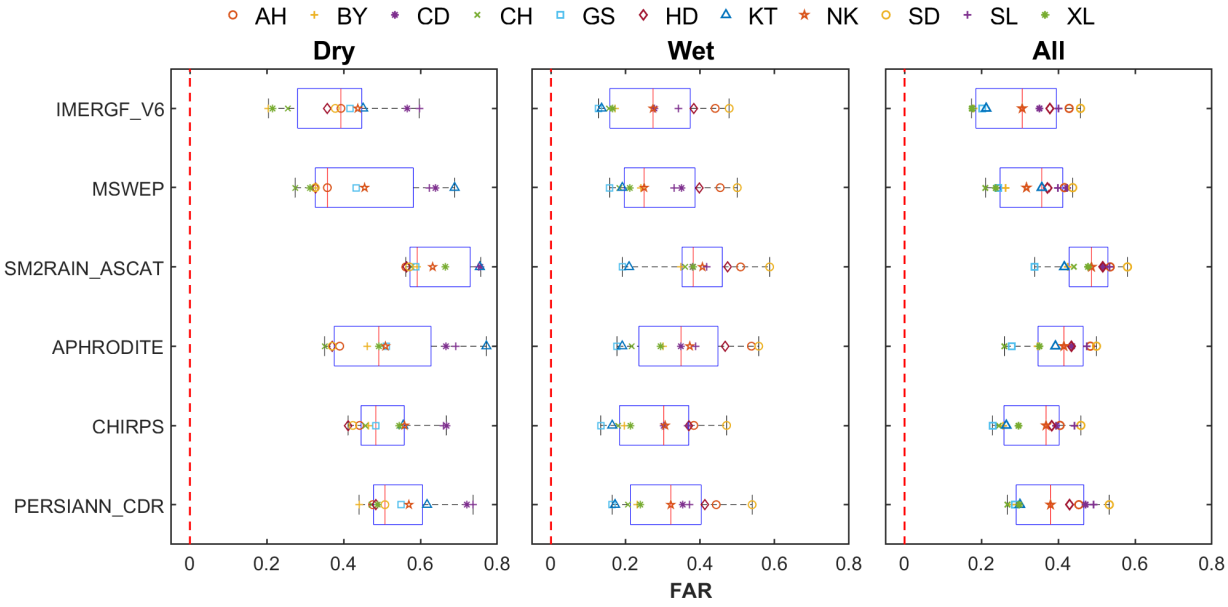
AH BY CD CH GS HD KT NK SD SL XL
Dry
Wet
All
IMERGF_V6
MSWEP
SM2RAIN_ASCAT
APHRODITE
CHIRPS
PERSIANN_CDR
0 0.2 0.4 0.6 0.8
0 0.2 0.4 0.6 0.8
0 0.2 0.4 0.6 0.8
FAR

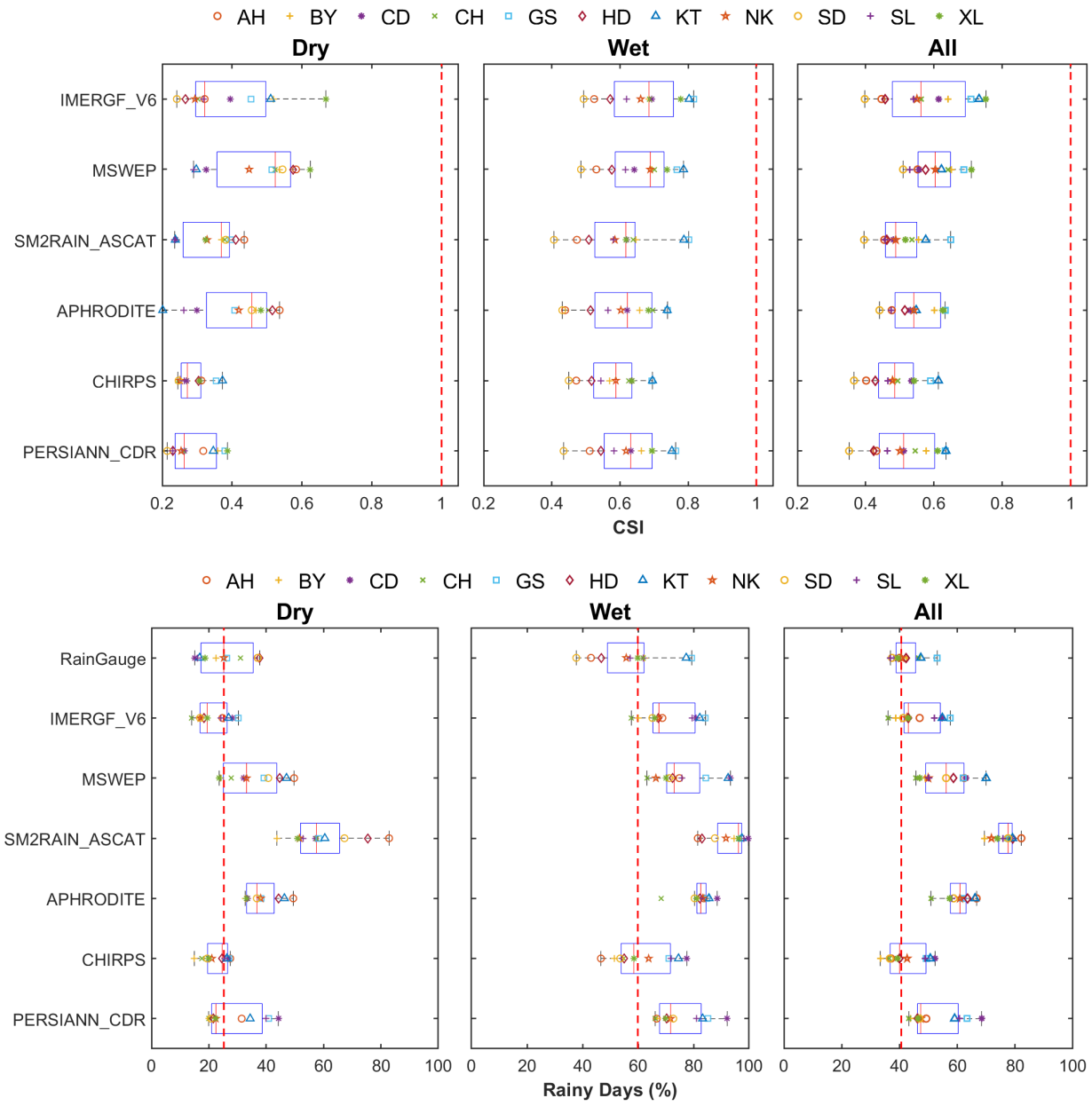

322

323 **Fig. 9.** The SPPs comparison using POD, FAR, CSI, and rainy–days detection (%) for annual, dry, and wet
324 seasons. Red dashed line shows the best value.

325 **Table 5.** The median performance measures of the SPPs are derived from daily precipitation measurements
326 obtained from rain gauges spanning the period 2007–2015. The most outstanding score is indicated by bold
327 values. A higher value corresponds to better performance, except for the metrics RMSE and FAR.

Metric	IMERGF	MSWEP	SM2RAIN –ASCAT	APHRODITE	CHIRPS	PERSIANN–CDR

	Dry	0.597	0.771	**0.873**	0.739	0.414	0.499
POD	Wet	0.901	0.921	**0.989**	0.917	0.767	0.886
	All	0.746	0.872	**0.954**	0.849	0.663	0.741
	Dry	0.393	**0.358**	0.592	0.492	0.484	0.507
FAR	Wet	**0.250**	0.274	0.381	0.349	0.303	0.322
	All	**0.306**	0.357	0.487	0.415	0.368	0.380
	Dry	0.321	**0.524**	0.369	0.456	0.272	0.263
CSI	Wet	**0.689**	0.685	0.617	0.621	0.588	0.632
	All	0.562	**0.604**	0.488	0.541	0.485	0.511
	Dry	**0.680**	0.413	0.425	0.415	0.301	0.347
CC	Wet	**0.718**	0.530	0.515	0.473	0.369	0.386
	All	**0.703**	0.547	0.540	0.520	0.436	0.449
	Dry	– 0.103	0.048	**0.014**	– 0.027	– 0.137	0.106
RB	Wet	**– 0.017**	– 0.076	– 0.204	– 0.140	0.042	0.085
	All	**– 0.006**	– 0.047	– 0.168	– 0.177	– 0.029	0.156
	Dry	7.578	7.555	**5.369**	5.728	6.435	8.513
RMSE	Wet	**10.493**	13.146	11.880	13.098	14.752	14.462
	All	**8.302**	11.319	9.377	10.143	11.485	11.947

Figure 9 and Table 5 show the performance of SPPs using rainfall detection metrics. In general, IMERGF (median POD of 0.746–rank 4, median FAR of 0.306–rank 1, and median CSI of 0.562–rank 2) showed the highest overall performance than other SPPs for the annual and seasonal rainfall comparisons, consistent with findings of Kumar et al. (2022) and Le et al. (2020). This reflects the fidelity of the IMERG retrieval algorithms to detect rainfall events with high POD and low FAR scores (Huffman et al., 2015, 2018). The second best SPP is MSWEP (median POD of 0.872–rank 2, median FAR of 0.357–rank 2, median CSI of 0.604–rank 1), followed by APHRODITE (median POD of 0.849–rank 3, median FAR of

0.415–rank 5, median CSI of 0.541–rank 3), and PERSIANN–CDR (median POD of 0.741–rank 5, median FAR of 0.380–rank 4, median CSI of 0.511–rank 4).

For rainy days detection, CHIRPS showed the highest similarity compared to the rain gauges, followed by IMERGF (Fig. 9). We could see that 40.62% of the observation across chosen basins had rainfall events, this figure from CHIRPS accounted for 40.01% while other products such as IMERGF, PERSIANN–CDR, and MSWEP comprised 43.08%, 47.32%, and 56.12% of the entire period, respectively. APHRODITE overestimated (60.91%) the number of rainy days, while it is 77.57% for SM2RAIN–ASCAT. MSWEP showed a similar overestimation result compared to APHRODITE with 56.12%, indicating a need to perform re–calibration and –evaluation for this product's algorithm, although its high–frequency temporal rainfall sampling (every 3 hours) (Beck et al., 2017) (Fig. 9, and Table 1). During the dry season, SM2RAIN–ASCAT, APHRODITE, and MSWEP overestimated the rainy days, whereas other SPPs showed the underestimation in the same comparison, reflecting the difficulty of SPPs to detect the short–term rainfall events, especially for coastal regions, in which most of the rainfall events caused by heavy rainfall from tropical cyclones.

In general, SM2RAIN–ASCAT and APHRODITE highly overestimated the rainy days that could be expected due to their high values of POD (Table 5) in terms of seasonal rainfall. CHIRPS showed a high correlation for rainy days between dry and wet seasons compared to rain gauges (Fig. 9). IMERGF overestimated (7.61%) and underestimated (5.79%) the number of rainy days in the wet season and dry season, respectively (Fig. 9).

4.1.3. SPPs comparison using temporal dynamic metrics

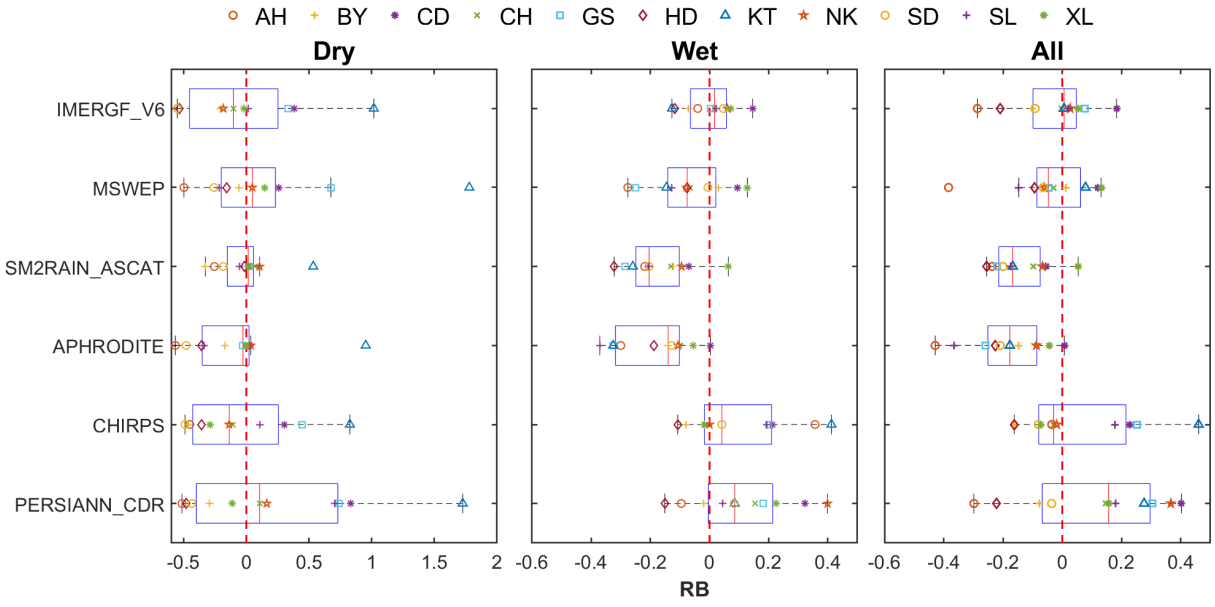

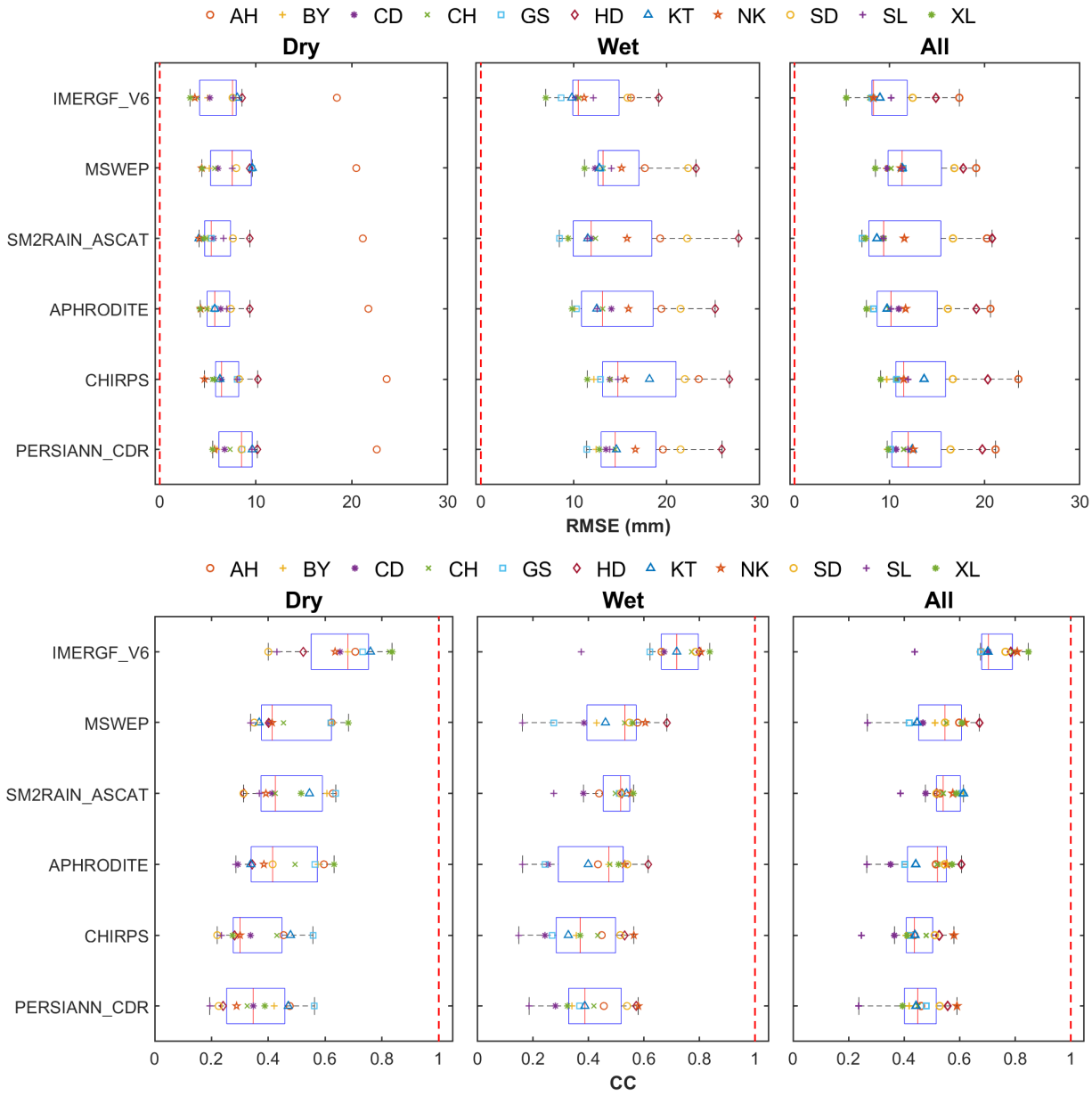

355 **Fig. 10.** The SPPs comparison using RB, RMSE, and CC derived from SPPs and rain gauge for annual,
356 dry, and wet seasons. Red dashed line shows the best value.

357 Figure 10 and Table 5 show the performance of SPPs using temporal dynamic metrics. In general,
358 IMERGF (median CC of 0.703–rank 1) showed the best overall CC score, followed by MSWEP (median
359 CC of 0.547–rank 2), SM2RAIN–ASCAT (median CC of 0.540–rank 3), and APHRODITE (median CC
360 of 0.520–rank 4). Other SPP products showed moderate median scores with PERSIANN–CDR (median
361 CC of 0.449–rank 5) and CHIRPS (median CC of 0.436–rank 6) (Table 5).

362 IMERGF showed the lowest RB score (median RB of – 0.006–rank 1) (Table 5). This product was
363 followed by CHIRPS (median RB of – 0.029–rank 2), MSWEP (median RB of – 0.047–rank 3), and other

SPPs (PERSIANN–CDR, SM2RAIN–ASCAT, and APHRODITE) with a lower RB scores (Table 5). These results are consistent with the findings of Le et al. (2020) and Beck et al. (2019a). IMERGF was ranked as the best SPP to detect drought events, followed by CHIRPS with the second–highest RB score (median RB of – 0.029). SM2RAIN–ASCAT obtained a very good RB score in the dry season (median RB of 0.014) (Table 5), indicating its skill in detecting drought conditions during the dry season. In terms of RMSE, IMERGF (median RMSE of 8.302 $mm.d^{-1}$) showed the lowest RMSE score for annual rainfall estimate, followed by SM2RAIN–ASCAT (median RMSE of 9.377 $mm.d^{-1}$), and APHRODITE (median RMSE of 10.143 $mm.d^{-1}$).

There was no significant difference between the wet and dry seasons for seasonal detection. The average median values for CC and RB during the dry season were 0.439 and 0.186, respectively, while during the wet season, they were 0.463 and 0.130, respectively. Moreover, the SPPs' average RMSE was 7.910 $mm.d^{-1}$ during the dry season and lower than the wet season (14.890 $mm.d^{-1}$), indicating a lower rainfall variability during the dry season.

4.2. Hydrological assessment performed by SPPs and rain gauges

4.2.1. Streamflow simulations at daily and monthly scales

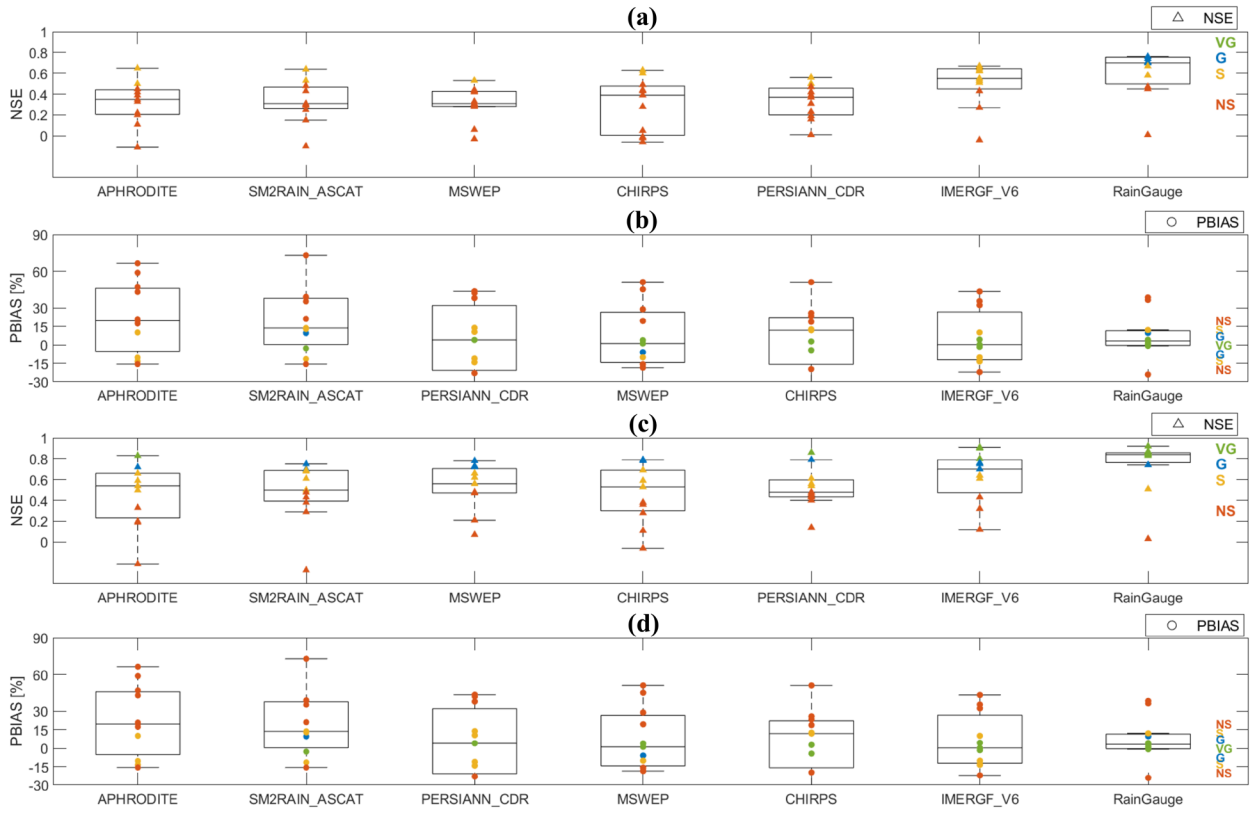

Fig. 11. The performance of SPPs for simulated streamflow, measured by NSE and PBIAS for (a, b) daily and (c, d) monthly streamflow using SWAT model, driven by rain gauges and different SPPs. Box plots show the median and interquartile range with outliers lying below or above the 10th and 90th percentiles, respectively. The color points represent the performance of each basin. The performance explanation: "VG" is Very Good, "G" is Good, "S" is Satisfactory, and "NS" is Not Satisfactory. The evaluation period: Cal. Calibration (2009 – 2012), Val. Validation (2013 – 2015).

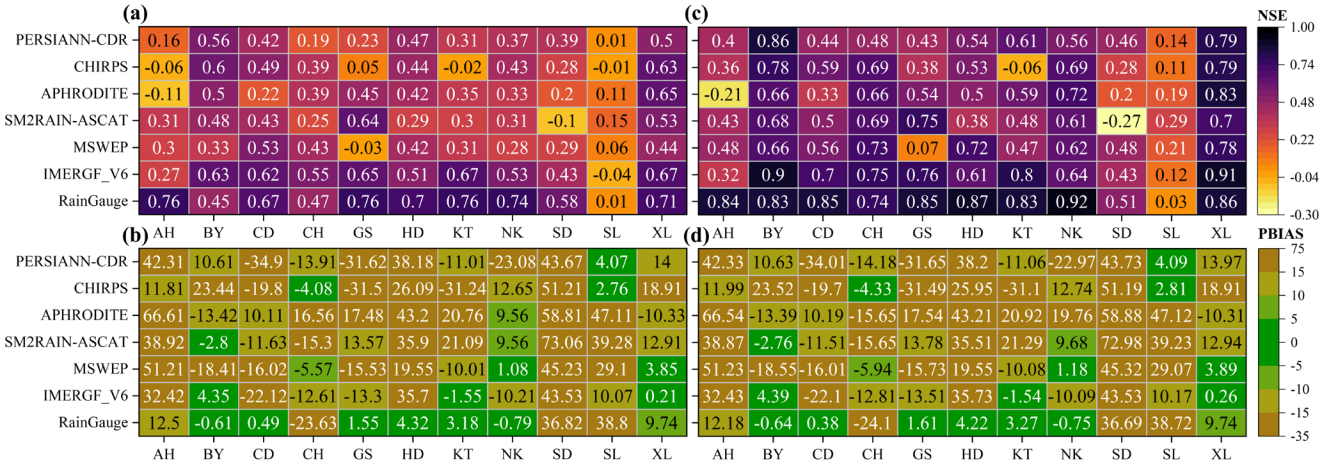

Fig. 12. Heat maps with the NSE and PBIAS scores for (a, b) daily and (c, d) monthly streamflow, respectively, using SWAT simulations, driven by rain gauges and different SPPs, at eleven basins.

For daily simulation, rain gauges (median NSE of – 0.70) showed the best overall performance, followed by IMERGF (median NSE of 0.55), categorized as Satisfactory level (Fig. 12a) (Moriasi et al., 2007). IMERGF showed better performances than the rain gauge in some basins (BY and CH), while other SPPs (CHIRPS, PERSIANN–CDR, APHRODITE, and MSWEP) showed poor performances (median NSE scores of 0.39, 0.37, 0.35, and 0.31, respectively) (Fig. 12a).

SPPs exhibited poor performances for cyclone–prone basin (AH) and semi–arid region (SL) while rain gauges only showed a good performance in cyclone–prone basin (Fig. 12). The performance of SM2RAIN–ASCAT was found to be comparable to rain gauges, in which it was found better than rain gauges in semi–arid region and was ranked as second best SPP (NSE score of 0.31) in cyclone–prone basin (AH), followed by MSWEP (NSE score of 0.30) (Fig. 12a).

For the PBIAS score, IMERGF (median PBIAS of 0.21%) showed the best overall performance, followed by MSWEP (median PBIAS of 1.08%), rain gauges (median PBIAS of 3.18%), and PERSIANN–CDR (4.07%) (Fig. 12b), categorized as Good level while APHRODITE (median PBIAS of 17.48%) showed a Not Satisfactory level (Table 2) (Moriasi et al., 2007).

403 The monthly streamflow simulation has shown better skills for hydrological simulations driven by
404 SPPs. For the monthly NSE score, rain–gauge–driven simulations (median NSE of 0.84) remained the best
405 overall performance, followed by IMERGF (median NSE of 0.70) (Fig. 12c). However, IMERGF showed
406 similar or slightly better model performances compared to the rain gauge in the S1 (XL and BY), S2 (CH)
407 and S6 (KT), indicating it as a potential alternative to rain gauges in monthly streamflow simulation.

408 MSWEP (median NSE of 0.56) showed good results in S1 (XL and BY), S2 (CH), and S7 (CD) and
409 outperformed IMEGRF in S4 (HD and SD) (Fig. 12c). APHRODITE (median NSE of 0.54) showed similar
410 results compared to CHIRPS (median NSE of 0.53), in which they performed good in S1 and S2 regions
411 but showed less performance in small ($\leq$ 1000 km^2) basin in S4 region (SD) (Fig. 12). SM2RAIN–ASCAT
412 showed good performances in S1, S2, and S3 with monthly NSE scores of at least 0.61 (Fig. 12) but was
413 indicated as easily affected in basins that have high variations in rainfall patterns (i.e., KT–S6, and HD,
414 SD–S4) (Figs. 7 and 8).

415 In general, only rain gauge–, IMERGF– and MSWEP– driven models exhibited Good and Satisfactory
416 levels in monthly simulation in terms of NSE, while other SPPs showed poorer results (APHRODITE,
417 CHIRPS, SM2RAIN–ASCAT, and PERSIANN–CDR). However, SPPs showed low performance at AH
418 basin and our suggestion is to re–evaluate for SPP datasets in regions that are heavily affected by the tropical
419 cyclone and monsoon systems.

420 For the monthly PBIAS score, IMERGF (median PBIAS of 0.26%) showed the best overall
421 performance, followed by MSWEP (median PBIAS of 1.18%), rain gauges (median PBIAS of 3.27%), and
422 PERSIANN–CDR (4.09%) (Fig. 12d). CHIRPS (median PBIAS of 11.99%) and SM2RAIN–ASCAT
423 (median PBIAS of 13.78%) showed Satisfactory levels while APHRODITE (median PBIAS of 19.76%)
424 showed a Not Satisfactory level for PBIAS.

425 *4.2.2. Streamflow simulation driven by SPPs at different basin sizes*

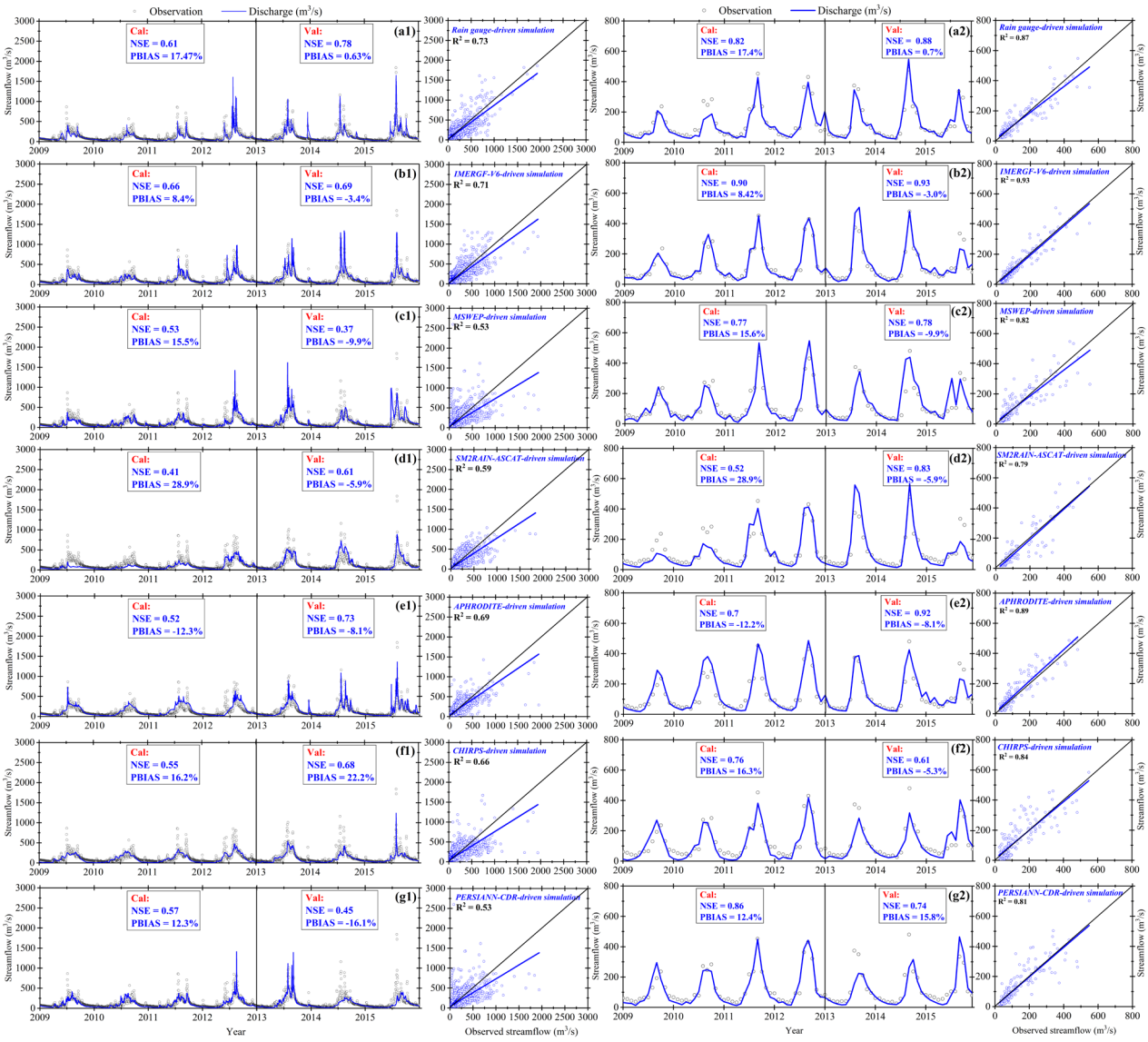

Fig. 13. The streamflow comparison in XL basin at (1) daily and (2) monthly scale between observed and simulated streamflow, driven by a) Rain gauges, b) IMERGF, c) MSWEP, d) SM2RAIN–ASCAT, e) APHRODITE, f) CHIRPS, and g) PERSIANN–CDR between 2007 and 2015. The Cal. Calibration (2009 – 2012), the Val. Validation (2013 – 2015).

The gauge–based simulations showed the best overall performance over eleven basins in terms of NSE and PBIAS scores at the largest basin – XL basin (6430 km^2) (Fig. 13). Other SPPs represented good scores which are lower in calibration and higher in the validation period (Fig. 13). IMERGF exhibited comparable results to the rain gauges in the daily simulation but outperformed the rain gauges in the monthly simulation.

We also considered the performance of SPPs over different basin sizes: large (> 4000 km^2), medium (≤ 4,000 km^2 and > 1000 km^2), and small (≤ 1000 km^2) and the observation (2009 – 2015) (Table 6).

Table 6. The median monthly NSE scores of SWAT models driven by rain gauges and SPPs are categorized by basin sizes. Change (in percentage) in NSE is calculated when the basin area decreases.

Basin size	Rain gauges	IMERGF	MSWEP	SM2RAIN–ASCAT	APHRODITE	CHIRPS	PERSIANN–CDR
Large	0.89	0.775	0.7	0.655	0.775	0.74	0.675
Medium	0.84	0.755	0.595	0.585	0.565	0.455	0.51
Small	0.83	0.43	0.48	0.43	0.2	0.36	0.44
Change in NSE (%)							
Large–Medium	– 5.61	– 2.58	– 15	– 10.68	– 27.09	– 38.51	– 24.44
Large–Small	– 6.74	– 44.51	– 31.40	– 34.35	– 74.19	– 51.35	– 34.81
Medium–Small	– 1.19	– 43.04	– 19.32	– 26.49	– 64.60	– 20.87	– 13.72

We found that (1) SPPs' streamflow performances decreased when the basins' area decreased. SPPs showed the best monthly streamflow performances in large basins but significantly decreased when the basin area decreased (Table 6); (2) CHIRPS showed the highest change of NSE when the basin area changed; (3) APHRODITE showed the highest decrease when basin area decreased from large to small; (4) SPPs showed at least 30% change in the model performance in terms of NSE; (5) IMERGF showed the best performance for streamflow simulation in large and medium size basins (Table 6 and Fig. 12).

4.2.4. SPPs performance in flood peak simulation at different basin sizes

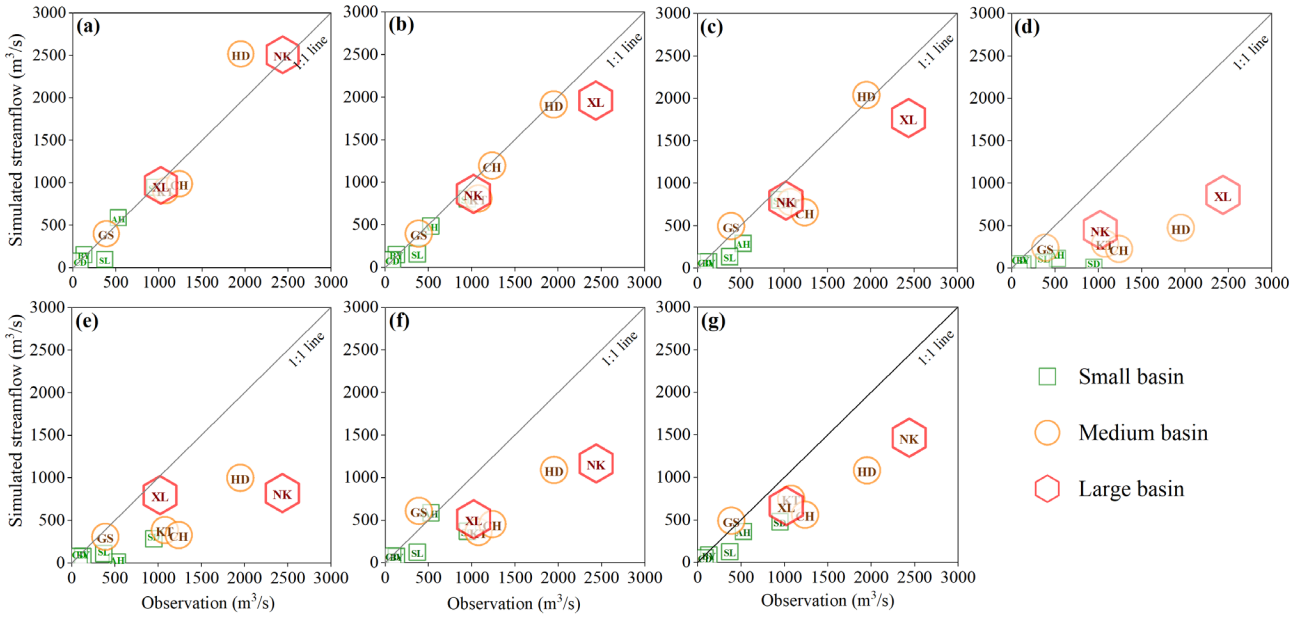

Fig. 14. The comparison of average flood peaks (2009 – 2015) at different basin sizes between observation and a) Rain gauges, b) IMERGF, c) MSWEP, d) SM2RAIN–ASCAT, e) APHRODITE, f) CHIRPS, and g) PERSIANN–CDR. The symbol's size represents the size of the catchment. The 1:1 represents the best match between simulated and observed flood peaks.

We used our CAFR framework to evaluate the performance of SPPs in simulating flood peaks in different basin sizes. Figure 14 represents the comparison between the SPP–driven average simulated flood peaks at large (> 4000 km^2), medium (≤ 4,000 km^2 and > 1000 km^2), and small (≤ 1000 km^2) basins and the observation (2009 – 2015). In general, rain gauges showed the best performance in simulating flood peaks over different basin sizes (Fig. 14a), followed by IMERGF (Fig. 14b) and MSWEP (Fig. 14c). Other SPPs showed underestimations of flood peaks, especially in medium and large size basins (Fig. 14). These results provided a better understanding of using these SPPs for flood forecasting in which flood forecasting models in conjunction with climate scenarios can be used to evaluate how these potential changes may impact the frequency, intensity, and geographic distribution of floods. This can be critical in informing decision–making for infrastructure, urban planning, and disaster response.

4.3. The correlation of SWAT simulations–performed by SPPs to rain gauges

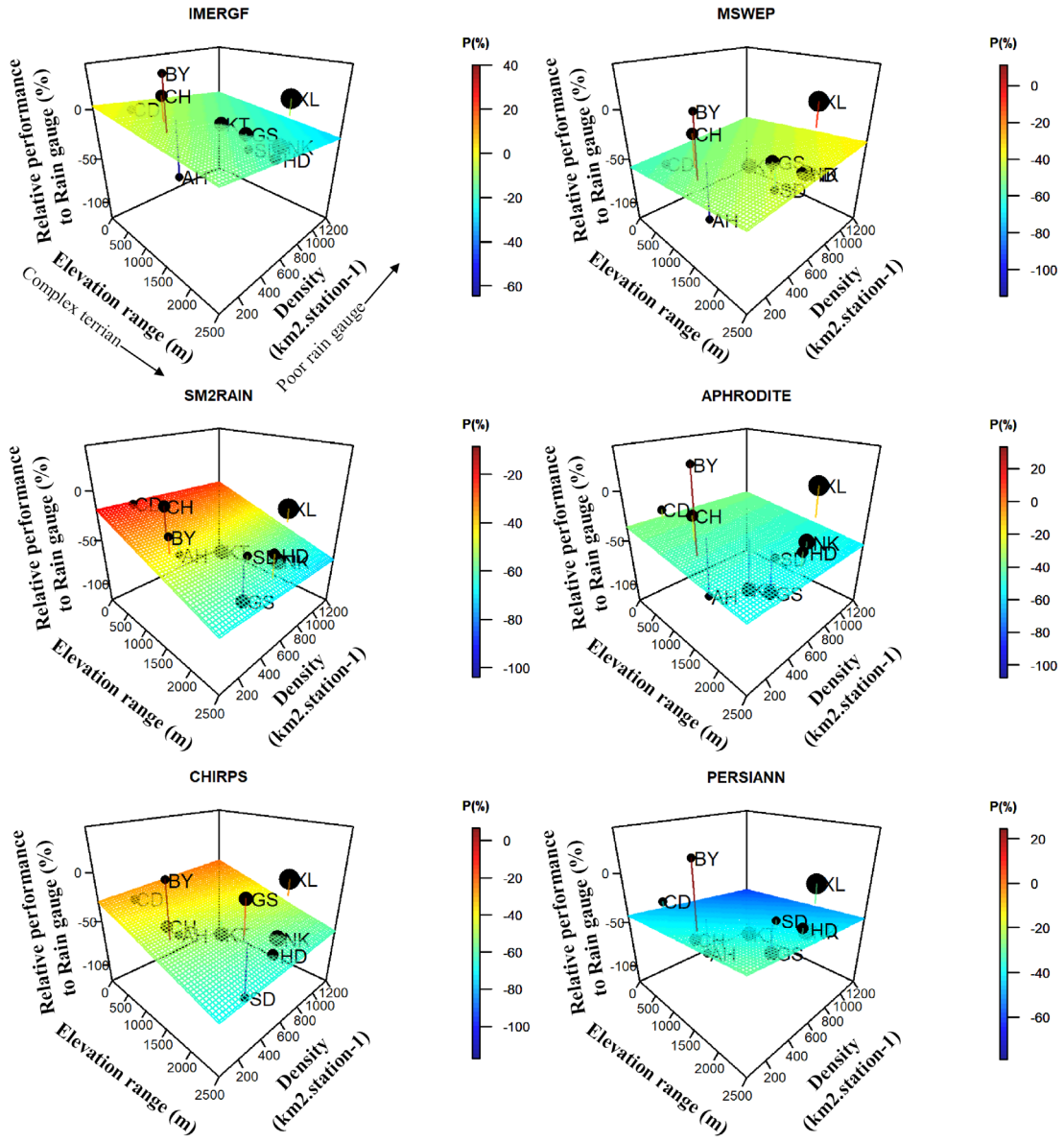

Fig. 15. Analysis of the bivariate relationship between SWAT simulations performed by SPPs and rain gauges, rain gauge density, and basin elevation range. The 3D plot represents the SPPs' performance trends relative to the rain gauge (P%). The size of the black dot represents the basin's dimensions.

IMEGRF performed best as all chosen basins showed the lowest deviation from rain gauges (Fig. 15). In contrast, PERSIANN–CDR and APHRODITE significantly differed in basin performance. Larger basins tended to have less rain gauges, and when SPP was used to simulate streamflow in large basins, the results were similar to those from rain gauges. Figure 15 indicated that low rain–gauge density exhibited high $P_{relative}$ values, consistent with the findings of Günter et al. (2013) and Le et al. (2020). It means hydrological simulations tend to perform better in watersheds with large storage capacities, and the because of the small

relative variance in these watersheds' streamflow, simulation results are superior to those of smaller watersheds.

4.4. CAFR ranking using the MCDM method

The MCDM programming method with the PROMETHEE I (partial ranking) and II (complete ranking) was used at the final stage of the CAFR framework to rank SPPs (see section 3.1).

Table 6. Summary of SPPs' ranking using the MCDM method.

Product	$\phi^+(x)$	$\phi^-(x)$	$\phi(x) = \phi^+(x) - \phi^-(x)$	Ranking
IMEGRF	3.862	1.137	2.725	1
MSWEP	2.862	2.068	0.794	2
SM2RAIN–ASCAT	2.62	2.379	0.241	3
APHRODITE	2.551	2.379	0.172	4
CHIRPS	1.586	3.379	– 1.793	5
PERSIANN–CDR	1.413	3.551	– 2.138	6

SPPs were ranked based on $\phi(x)$ values; the lowest value represents the worst–performing product, while the higher value represents a higher ranking. The calculated $\phi(x)$ values were analyzed from over–performed steps for each basin, not the average or median scores, to maintain the overall accuracy of this approach. All the metrics are equivalently treated in deriving the final rank index. We determined positive and negative outranking flows for each alternative, conducted a partial ranking, and calculated the net outranking flow for each alternative, resulting in the final ranking of SPPs. In general, IMERGF was the best, followed by MSWEP, SM2RAIN–ASCAT, APHRODITE, CHIRPS, and PERSIANN–CDR (Table 6).

4.5. Limitations and future study

We acknowledged that one of the limitations was the use of different spatial resolutions of SPPs. Additionally, we would consider extending the streamflow simulation, which was limited in this study due to the scarcity of observed streamflow and in situ precipitation data from meteorological stations. Our future works would aim to increase the performance of SPPs by applying bias correction techniques.

On the other hand, our future work will also involve verifying the accuracy of other hydrological variables, particularly soil moisture, using the latest data obtained from the 400 m and 1 km downscaled

Soil Moisture Active Passive (SMAP) (Fang et al., 2020, 2021a, 2021b, 2022). This variable has been shown to have an impact on hydrological simulation in various regions, including Vietnam (Le et al., 2020), Lower Mekong River Basin (Dandridge et al., 2020), and droughts in Australia (Fang et al., 2021a). The validation of hydrological models such as SWAT with soil moisture measurements will assist in refining the model's predictions of streamflow.

5. Conclusions

This study introduces the CAFR framework, which aims to evaluate the capabilities of using SPPs in hydrological models for streamflow simulation. The CAFR was tested in eleven basins with varying sizes throughout Vietnam's sub–climate regions. The main findings are summarized:

(1) IMERGF demonstrates the highest overall performance among all SPPs in simulating streamflow. It shows consistent rainfall estimates across different basin sizes, with the best performance observed in large basins. Flood peak simulations driven by IMERGF and MSWEP perform comparably to simulations driven by rain gauges.
(2) SM2RAIN–ASCAT exhibits the lowest rainfall bias (RB) score compared to rain gauges during the dry season, suggesting a good SPP for drought detection and analysis. It also shows the highest skill (NSE) in simulating streamflow in a semi–arid basin.
(3) The performance of SPP–driven streamflow simulations varies with basin size. SPPs perform best in terms of monthly streamflow in large basins, but the performance decreases significantly as the basin area decreases. The model performance, as measured by NSE, can vary by at least 30% across different SPPs.
(4) The CAFR provides a comprehensive ranking of SPPs by comparing their rainfall estimates with rain gauges and evaluating their performance in hydrological streamflow simulations. The performance of SPPs varies across regions, but CAFR resolves this variability and offers an optimal ranking.

This study's results show a more effective approach to understanding the application of SPPs in hydrological modeling. These results are useful for estimating water resources and supporting water management in Vietnam and Southeast Asia, and this framework could be applied to similar regions in other future works.

CRediT authorship contribution statement

Thanh–Nhan–Duc Tran: Conceptualization, Methodology, Software, Validation, Formal analysis, Investigation, Resources, Data curation, Writing – original draft, Writing – review & editing, Visualization. **Manh–Hung Le:** Conceptualization, Methodology, Formal analysis, Investigation, Resources, Data curation, Writing – review & editing, Visualization. **Runze Zhang:** Conceptualization, Formal analysis, Investigation, Resources, Data curation, Writing – review & editing, Visualization. **Binh Quang Nguyen:** Conceptualization, Methodology, Formal analysis, Investigation, Resources, Data curation, Writing – review & editing, Visualization. **John Bolten:** Investigation, Resources, Project administration, Funding acquisition, Writing – review & editing. **Venkataraman Lakshmi:** Supervision, Project administration, Funding acquisition, Writing – review & editing.

Declaration of Competing Interest

We declare that the work presented in this article is not influenced by any personal or financial relationships.

Acknowledgments

This project received funding from the University of Virginia, Charlottesville, VA, the U.S. We sincerely thank the institutions for granting us access to the in-situ data critical for this study. We extend our gratitude to NASA, the Climate Hazards Group at the University of California, Santa Barbara, the Center for Hydrometeorology and Remote Sensing at the University of California, Irvine, the authors of the Soil Moisture to Rain and Multi–Source Weighted–Ensemble Precipitation for providing access to the SPP products. We also thank the Vietnam Meteorological and Hydrological Administration for rain gauge and streamflow observations. Furthermore, we wish to acknowledge the anonymous reviewers for their valuable feedback and recommendations, which have enhanced the quality of this paper.

References

Abbaspour, K. C., Yang, J., Maximov, I., Siber, R., Bogner, K., Mieleitner, J., Zobrist, J., & Srinivasan, R. (2007). Modelling hydrology and water quality in the pre-alpine/alpine Thur watershed using SWAT. Journal of Hydrology, 333(2–4), 413–430. https://doi.org/10.1016/j.jhydrol.2006.09.014

Abbaspour, K. C., Rouholahnejad, E., Vaghefi, S., Srinivasan, R., Yang, H., & Kløve, B. (2015). A continental-scale hydrology and water quality model for Europe: Calibration and uncertainty of a high-resolution large-scale SWAT model. Journal of Hydrology, 524, 733–752. https://doi.org/10.1016/j.jhydrol.2015.03.027

Alijanian, M., Rakhshandehroo, G. R., Mishra, A. K., & Dehghani, M. (2017). Evaluation of satellite rainfall climatology using CMORPH, PERSIANN-CDR, PERSIANN, TRMM, MSWEP over Iran. International Journal of Climatology, 37(14), 4896–4914. https://doi.org/10.1002/joc.5131

Anjum, M. N., Irfan, M., Waseem, M., Leta, M. K., Niazi, U. M., Rahman, S. U., Ghanim, A., Mukhtar, M. A., & Nadeem, M. U. (2022). Assessment of PERSIANN-CCS, PERSIANN-CDR, SM2RAIN-ASCAT, and CHIRPS-2.0 Rainfall Products over a Semi-Arid Subtropical Climatic Region. Water (Switzerland), 14(2). https://doi.org/10.3390/w14020147

Arnold, J. G., Moriasi, D. N., Gassman, P. W., Abbaspour, K. C., White, M. J., Srinivasan, R., Santhi, C., Harmel, R. D., Van Griensven, A., Van Liew, M. W., Kannan, N., & Jha, M. K. (2012). SWAT: Model use, calibration, and validation. Transactions of the ASABE, 55(4), 1491–1508.

Ahmed, K., Shahid, S., Wang, X., Nawaz, N., & Najeebullah, K. (2019). Evaluation of gridded precipitation datasets over arid regions of Pakistan. Water (Switzerland), 11(2). https://doi.org/10.3390/w11020210

Ashouri, H., Hsu, K. L., Sorooshian, S., Braithwaite, D. K., Knapp, K. R., Cecil, L. D., Nelson, B. R., & Prat, O. P. (2015). PERSIANN-CDR: Daily precipitation climate data record from multisatellite observations for hydrological and climate studies. Bulletin of the American Meteorological Society, 96(1), 69–83. https://doi.org/10.1175/BAMS-D-13-00068.1

Ashrafi, S., Kerachian, R., Pourmoghim, P., Behboudian, M., & Motlaghzadeh, K. (2022a). Evaluating and improving the sustainability of ecosystem services in river basins under climate change. Science of the Total Environment, 806. https://doi.org/10.1016/j.scitotenv.2021.150702

Ashrafi, S., Khoie, M. M. M., Kerachian, R., & Shafiee-Jood, M. (2022b). Managing basin-wide ecosystem services using the bankruptcy theory. Science of the Total Environment, 842(June).

https://doi.org/10.1016/j.scitotenv.2022.156845

Beck, H. E., Van Dijk, A. I. J. M., Levizzani, V., Schellekens, J., Miralles, D. G., Martens, B., & De Roo, A. (2017). MSWEP: 3-hourly 0.25° global gridded precipitation (1979-2015) by merging gauge, satellite, and reanalysis data. Hydrology and Earth System Sciences, 21(1), 589–615. https://doi.org/10.5194/hess-21-589-2017

Beck, H. E., Pan, M., Roy, T., Weedon, G. P., Pappenberger, F., Van Dijk, A. I. J. M., Huffman, G. J., Adler, R. F., & Wood, E. F. (2019a). Daily evaluation of 26 precipitation datasets using Stage-IV gauge-radar data for the CONUS. Hydrology and Earth System Sciences, 23(1), 207–224. https://doi.org/10.5194/hess-23-207-2019

Beck, H. E., Wood, E. F., Pan, M., Fisher, C. K., Miralles, D. G., Van Dijk, A. I. J. M., McVicar, T. R., & Adler, R. F. (2019b). MSWEP v2 Global 3-hourly 0.1° precipitation: Methodology and quantitative assessment. Bulletin of the American Meteorological Society, 100(3), 473–500. https://doi.org/10.1175/BAMS-D-17-0138.1

Beck, H. E., Vergopolan, N., Pan, M., Levizzani, V., van Dijk, A. I. J. M., Weedon, G. P., Brocca, L., Pappenberger, F., Huffman, G. J., & Wood, E. F. (2020). Global-scale evaluation of 22 precipitation datasets using gauge observations and hydrological modeling. Advances in Global Change Research, 69, 625–653. https://doi.org/10.1007/978-3-030-35798-6_9

Behboudian, M., Kerachian, R., Motlaghzadeh, K., & Ashrafi, S. (2021). Evaluating water resources management scenarios considering the hierarchical structure of decision-makers and ecosystem services-based criteria. Science of the Total Environment, 751. https://doi.org/10.1016/j.scitotenv.2020.141759

Behzadian, M., Kazemzadeh, R. B., Albadvi, A., & Aghdasi, M. (2010). PROMETHEE: A comprehensive literature review on methodologies and applications. European Journal of Operational Research, 200(1), 198–215. https://doi.org/10.1016/j.ejor.2009.01.021

Brans, J. P., Vincke, P., & Mareschal, B. (1986). How to select and how to rank projects : The PROMETHEE method . European Journal of Operational Research 14 ... How to select and how to rank projects : The PROMETHEE method. European Journal of Operational Research, 24, 228–238.

Brocca, L., Hasenauer, S., Kidd, R., Dorigo, W., Wagner, W., & Levizzani, V. (2014). Soil as a natural rain gauge: Estimating global rainfall from satellite soil moisture data. Journal of Geophysical Research: Atmospheres, 5128–5141. https://doi.org/10.1002/2014JD021489

Brocca, L., Filippucci, P., Hahn, S., Ciabatta, L., Massari, C., Camici, S., Schüller, L., Bojkov, B., & Wagner, W. (2019). SM2RAIN-ASCAT (2007-2018): Global daily satellite rainfall data from ASCAT soil moisture observations. Earth System Science Data, 11(4), 1583–1601. https://doi.org/10.5194/essd-11-1583-2019

Chen, C. J., Senarath, S. U. S., Dima-West, I. M., & Marcella, M. P. (2017). Evaluation and restructuring of gridded precipitation data over the Greater Mekong Subregion. International Journal of Climatology, 37(1), 180–196. https://doi.org/10.1002/joc.4696

Chang, C., Lee, H., Do, S. K., Du, T. L. T., Markert, K., Hossain, F., Khalique, S., Piman, T., Meechaiya, C., Bui, D. D., Bolten, J. D., Hwang, E., & Chul, H. (2023). Operational forecasting inundation extents using REOF analysis (FIER) over lower Mekong and its potential economic impact on agriculture. Environmental Modelling and Software, 162(August 2022), 105643. https://doi.org/10.1016/j.envsoft.2023.105643

Du, T. L. T., Lee, H., Bui, D. D., Graham, L. P., Darby, S. D., Pechlivanidis, I. G., Leyland, J., Biswas, N. K., Choi, G., Batelaan, O., Bui, T. T. P., Do, S. K., Tran, T. V., Nguyen, H. T., & Hwang, E. (2022). Streamflow Prediction in Highly Regulated, Transboundary Watersheds Using Multi-Basin Modeling and Remote Sensing Imagery. Water Resources Research, 58(3), 1–25. https://doi.org/10.1029/2021WR031191

Dandridge, C., Lakshmi, V., Bolten, J., & Srinivasan, R. (2019). Evaluation of satellite-based rainfall estimates in the Lower Mekong River Basin (Southeast Asia). Remote Sensing, 11(22), 1–17. https://doi.org/10.3390/rs11222709

Dandridge, C., Fang, B., & Lakshmi, V. (2020). Downscaling of SMAP Soil Moisture in the Lower Mekong River Basin. Water (Switzerland), 12(1). https://doi.org/10.3390/w12010056

Derin, Y., & Yilmaz, K. K. (2014). Evaluation of multiple satellite-based precipitation products over complex topography. Journal of Hydrometeorology, 15(4), 1498–1516. https://doi.org/10.1175/JHM-D-13-0191.1

Dile, Y. T., Daggupati, P., George, C., Srinivasan, R., & Arnold, J. (2016). Introducing a new open source GIS user interface for the SWAT model. Environmental Modelling and Software, 85(September), 129–138. https://doi.org/10.1016/j.envsoft.2016.08.004

Do, H. X., Le, M. H., Pham, H. T., Le, T. H., & Nguyen, B. Q. (2022). Identifying hydrologic reference stations to understand changes in water resources across Vietnam-a data-driven approach. Vietnam Journal of Earth Sciences, 44(1), 145–165. https://doi.org/10.15625/2615-9783/16980

Fayne, J. V., Bolten, J. D., Doyle, C. S., Fuhrmann, S., Rice, M. T., Houser, P. R., & Lakshmi, V. (2017). Flood mapping in the lower Mekong River Basin using daily MODIS observations. International Journal of Remote Sensing, 38(6), 1737–1757. https://doi.org/10.1080/01431161.2017.1285503

Fang, B., Kansara, P., Dandridge, C., & Lakshmi, V. (2021a). Drought monitoring using high spatial resolution soil moisture data over Australia in 2015–2019. Journal of Hydrology, 594(July 2020), 125960. https://doi.org/10.1016/j.jhydrol.2021.125960

Fang, B., Lakshmi, V., Bindlish, R., Jackson, T. J., & Liu, P. W. (2020). Evaluation and validation of a high spatial resolution satellite soil moisture product over the Continental United States. Journal of Hydrology, 588(April), 125043. https://doi.org/10.1016/j.jhydrol.2020.125043

Fang, B., Lakshmi, V., Cosh, M., & Hain, C. (2021b). Very High Spatial Resolution Downscaled SMAP Radiometer Soil Moisture in the CONUS Using VIIRS/MODIS Data. IEEE Journal of Selected Topics in Applied Earth Observations and Remote Sensing, 14, 4946–4965. https://doi.org/10.1109/JSTARS.2021.3076026

Fang, B., Lakshmi, V., Cosh, M., Liu, P. W., Bindlish, R., & Jackson, T. J. (2022). A global 1-km downscaled SMAP soil moisture product based on thermal inertia theory. Vadose Zone Journal, 21(2), 1–27. https://doi.org/10.1002/vzj2.20182

Funk, C., Peterson, P., Landsfeld, M., Pedreros, D., Verdin, J., Shukla, S., Husak, G., Rowland, J., Harrison, L., Hoell, A., & Michaelsen, J. (2015). The climate hazards infrared precipitation with stations - A new environmental record for monitoring extremes. Scientific Data, 2, 1–21. https://doi.org/10.1038/sdata.2015.66

Gerlak, A. K., Lautze, J., & Giordano, M. (2011). Water resources data and information exchange in transboundary water treaties. International Environmental Agreements: Politics, Law and Economics, 11(2), 179–199. https://doi.org/10.1007/s10784-010-9144-4

Günter, B., Sivapalan, M., Wagener, T., Viglione, A., & Savenije, H. (2013). Runoff Prediction in Ungauged Basins: Synthesis across Processes, Places and Scales. Cambridge University Press.

Hou, A. Y., Kakar, R. K., Neeck, S., Azarbarzin, A. A., Kummerow, C. D., Kojima, M., Oki, R., Nakamura, K., & Iguchi, T. (2014). The global precipitation measurement mission. Bulletin of the American Meteorological Society, 95(5), 701–722. https://doi.org/10.1175/BAMS-D-13-00164.1

Hsu, K. L., Gao, X., Sorooshian, S., & Gupta, H. V. (1997). Precipitation estimation from remotely sensed information using artificial neural networks. Journal of Applied Meteorology, 36(9), 1176–

672 1190. https://doi.org/10.1175/1520-0450(1997)036<1176:PEFRSI>2.0.CO;2

673 Huffman, G. J., Bolvin, D. T., Braithwaite, D., Hsu, K., Joyce, R., Kidd, C., Nelkin, E. J., & Xie, P.
674 (2015). NASA Global Precipitation Measurement (GPM) Integrated Multi-satellitE Retrievals for
675 GPM (IMERG). Algorithm Theoretical Basis Document (ATBD) Version 4.5, November, 26.
676 https://pmm.nasa.gov/sites/default/files/imce/times_allsat.jpg%0Ahttps://pmm.nasa.gov/sites/default
677 /files/document_files/IMERG_ATBD_V4.5.pdf%0Ahttps://pmm.nasa.gov/sites/default/files/docum
678 ent_files/IMERG_ATBD_V4.5.pdf

679 Huffman, G. J., Bolvin, D. T., & Nelkin, E. J. (2018). Integrated Multi-satellitE Retrievals for GPM
680 (IMERG) Technical Documentation.

681 Iqbal, Z., Shahid, S., Ahmed, K., Wang, X., Ismail, T., & Gabriel, H. F. (2022). Bias correction method of
682 high-resolution satellite-based precipitation product for Peninsular Malaysia. Theoretical and
683 Applied Climatology, 148(3–4), 1429–1446. https://doi.org/10.1007/s00704-022-04007-6

684 Ji, X., Li, Y., Luo, X., He, D., Guo, R., Wang, J., Bai, Y., Yue, C., & Liu, C. (2020). Evaluation of bias
685 correction methods for APHRODITE data to improve hydrologic simulation in a large Himalayan
686 basin. Atmospheric Research, 242(April), 104964. https://doi.org/10.1016/j.atmosres.2020.104964

687 Kumar, S., Amarnath, G., Ghosh, S., Park, E., Baghel, T., Wang, J., Pramanik, M., & Belbase, D. (2022).
688 Assessing the Performance of the Satellite-Based Precipitation Products (SPP) in the Data-Sparse
689 Himalayan Terrain. Remote Sensing, 14(19), 4810. https://doi.org/10.3390/rs14194810

690 Lai, S., Xie, Z., Bueh, C., & Gong, Y. (2020). Fidelity of the APHRODITE Dataset in Representing
691 Extreme Precipitation over Central Asia. Advances in Atmospheric Sciences, 37(12), 1405–1416.
692 https://doi.org/10.1007/s00376-020-0098-3

693 Lauri, H., Räsänen, T. A., & Kummu, M. (2014). Using Reanalysis and Remotely Sensed Temperature
694 and Precipitation Data for Hydrological Modeling in Monsoon Climate: Mekong River Case Study.
695 Journal of Hydrometeorology, 15(4), 1532–1545. https://doi.org/10.1175/jhm-d-13-084.1

696 Le, M. H., Sutton, J. R. P., Bui, D. Du, Bolten, J. D., & Lakshmi, V. (2018). Comparison and bias
697 correction of TMPA precipitation products over the lower part of Red-Thai Binh River Basin of
698 Vietnam. Remote Sensing, 10(10). https://doi.org/10.3390/rs10101582

699 Le, M. H., Lakshmi, V., Bolten, J., & Bui, D. Du. (2020). Adequacy of Satellite-derived Precipitation
700 Estimate for Hydrological Modeling in Vietnam Basins. Journal of Hydrology, 586(March), 124820.
701 https://doi.org/10.1016/j.jhydrol.2020.124820

Libertino, A., Sharma, A., Lakshmi, V., & Claps, P. (2016). A global assessment of the timing of extreme rainfall from TRMM and GPM for improving hydrologic design. Environmental Research Letters, 11(5). https://doi.org/10.1088/1748-9326/11/5/054003

Li, H., Haugen, J. E., & Xu, C. Y. (2018). Precipitation pattern in the Western Himalayas revealed by four datasets. Hydrology and Earth System Sciences, 22(10), 5097–5110. https://doi.org/10.5194/hess-22-5097-2018

McIntyre, N., Lee, H., Wheater, H., Young, A., & Wagener, T. (2005). Ensemble predictions of runoff in ungauged catchments. Water Resources Research, 41(12), 1–14. https://doi.org/10.1029/2005WR004289

Michaelides, S., Levizzani, V., Anagnostou, E., Bauer, P., Kasparis, T., & Lane, J. E. (2009). Precipitation: Measurement, remote sensing, climatology and modeling. Atmospheric Research, 94(4), 512–533. https://doi.org/10.1016/j.atmosres.2009.08.017

Mondal, A., Lakshmi, V., & Hashemi, H. (2018). Intercomparison of trend analysis of Multisatellite Monthly Precipitation Products and Gauge Measurements for River Basins of India. Journal of Hydrology, 565(April), 779–790. https://doi.org/10.1016/j.jhydrol.2018.08.083

Mohammed, I. N., Bolten, J. D., Srinivasan, R., & Lakshmi, V. (2018a). Improved hydrological decision support system for the Lower Mekong River Basin using satellite-based earth observations. Remote Sensing, 10(6). https://doi.org/10.3390/rs10060885

Mohammed, I. N., Bolten, J. D., Srinivasan, R., & Lakshmi, V. (2018b). Satellite observations and modeling to understand the Lower Mekong River Basin streamflow variability. Journal of Hydrology, 564(July), 559–573. https://doi.org/10.1016/j.jhydrol.2018.07.030

Mohammed, I. N., Bolten, J. D., Srinivasan, R., Meechaiya, C., Spruce, J. P., & Lakshmi, V. (2018c). Ground and satellite based observation datasets for the Lower Mekong River Basin. Data in Brief, 21(2018), 2020–2027. https://doi.org/10.1016/j.dib.2018.11.038

Moriasi, D. N., J. G. Arnold, M. W. Van Liew, R. L. Bingner, R. D. Harmel, & T. L. Veith. (2007). Model Evaluation Guidelines for Systematic Quantification of Accuracy in Watershed Simulations. Transactions of the ASABE, 50(3), 885–900. https://doi.org/10.13031/2013.23153

Moriasi, D. N., Gitau, M. W., Pai, N., & Daggupati, P. (2015). Hydrologic and water quality models: Performance measures and evaluation criteria. Transactions of the ASABE, 58(6), 1763–1785. https://doi.org/10.13031/trans.58.10715

National Institute for Soils and Fertilizers. (2002). The basic information of main soil units of Vietnam. The Gioi Publishers.

Nguyen-Xuan, T., Ngo-Duc, T., Kamimera, H., Trinh-Tuan, L., Matsumoto, J., Inoue, T., & Phan-Van, T. (2016). The Vietnam Gridded Precipitation (VnGP) Dataset: Construction and Validation. Sola, 12(0), 291–296. https://doi.org/10.2151/sola.2016-057

Nguyen, B. Q., Kantoush, S., binh, D. Van, Saber, M., Vo, D. N., & Sumi, T. (2022a). Understanding the anthropogenic development impacts on long-term flow regimes in a tropical river basin, Central Vietnam. Hydrological Sciences Journal, null-null. https://doi.org/10.1080/02626667.2022.2153298

Nguyen, B. Q., Tran, T., Łukaszewska, M. G.-, Sinicyn, G., & Lakshmi, V. (2022b). Assessment of Urbanization-Induced Land-Use Change and Its Impact on Temperature, Evaporation, and Humidity in Central Vietnam. 1–24.

Nguyen, B. Q., Kantoush, S., Binh, D. Van, Saber, M., Vo, D. N., & Sumi, T. (2023). Quantifying the impacts of hydraulic infrastructure on tropical streamflows. Hydrological Processes, 37(3). https://doi.org/https://doi.org/10.1002/hyp.14834

Nguyen, D. N., & Nguyen, T. H. (2004). Climate and Climate Resources in Vietnam (in Vietnamese). Agricultural Publishing House.

Nguyen, T. V., Dietrich, J., Dang, T. D., Tran, D. A., Van Doan, B., Sarrazin, F. J., Abbaspour, K., & Srinivasan, R. (2022). An interactive graphical interface tool for parameter calibration, sensitivity analysis, uncertainty analysis, and visualization for the Soil and Water Assessment Tool. Environmental Modelling and Software, 156(August). https://doi.org/10.1016/j.envsoft.2022.105497

Nhi, P. T. T., Khoi, D. N., & Hoan, N. X. (2019). Evaluation of five gridded rainfall datasets in simulating streamflow in the upper Dong Nai river basin, Vietnam. International Journal of Digital Earth, 12(3), 311–327. https://doi.org/10.1080/17538947.2018.1426647

Oals, C. H. G. (2011). WATERSHED DELINEATION USING TAUDEM. A tutorial for using TauDEM to delineate a single watershed. August, 1–16.

Paredes-Trejo, F., Barbosa, H. A., & Spatafora, L. R. (2018). Assessment of SM2RAIN-derived and state-of-the-art satellite rainfall products over Northeastern Brazil. Remote Sensing, 10(7). https://doi.org/10.3390/rs10071093

Paredes-Trejo, F., Barbosa, H., & dos Santos, C. A. C. (2019). Evaluation of the performance of

762 SM2RAIN-derived rainfall products over Brazil. Remote Sensing, 11(9), 1–28.
763 https://doi.org/10.3390/rs11091113

764 Plengsaeng, B., Wehn, U., & van der Zaag, P. (2014). Data-sharing bottlenecks in transboundary
765 integrated water resources management: a case study of the Mekong River Commission's
766 procedures for data sharing in the Thai context. Water International, 39(7), 933–951.
767 https://doi.org/10.1080/02508060.2015.981783

768 Rahman, K. U., Shang, S., Shahid, M., & Wen, Y. (2019). Performance assessment of SM2RAIN-CCI
769 and SM2RAIN-ASCAT precipitation products over Pakistan. Remote Sensing, 11(17).
770 https://doi.org/10.3390/rs11172040

771 Ren, P., Li, J., Feng, P., Guo, Y., & Ma, Q. (2018). Evaluation of multiple satellite precipitation products
772 and their use in hydrological modelling over the Luanhe River Basin, China. Water (Switzerland),
773 10(6). https://doi.org/10.3390/w10060677

774 Shen, Z., Yong, B., Gourley, J. J., Qi, W., Lu, D., Liu, J., Ren, L., Hong, Y., & Zhang, J. (2020). Recent
775 global performance of the Climate Hazards group Infrared Precipitation (CHIRP) with Stations
776 (CHIRPS). Journal of Hydrology, 591(July), 125284. https://doi.org/10.1016/j.jhydrol.2020.125284

777 Sunilkumar, K., Yatagai, A., & Masuda, M. (2019). Preliminary Evaluation of GPM-IMERG Rainfall
778 Estimates Over Three Distinct Climate Zones With APHRODITE. Earth and Space Science, 6(8),
779 1321–1335. https://doi.org/10.1029/2018EA000503

780 Tan, M. L., & Santo, H. (2018). Comparison of GPM IMERG, TMPA 3B42 and PERSIANN-CDR
781 satellite precipitation products over Malaysia. Atmospheric Research, 202(July 2017), 63–76.
782 https://doi.org/10.1016/j.atmosres.2017.11.006

783 Tang, X., Zhang, J., Wang, G., Yang, Q., Yang, Y., Guan, T., Liu, C., Jin, J., Liu, Y., & Bao, Z. (2019).
784 Evaluating Suitability of Multiple Precipitation Products for the Lancang River Basin. Chinese
785 Geographical Science, 29(1), 37–57. https://doi.org/10.1007/s11769-019-1015-5

786 Tapiador, F. J., Turk, F. J., Petersen, W., Hou, A. Y., García-Ortega, E., Machado, L. A. T., Angelis, C.
787 F., Salio, P., Kidd, C., Huffman, G. J., & de Castro, M. (2012). Global precipitation measurement:
788 Methods, datasets and applications. Atmospheric Research, 104–105, 70–97.
789 https://doi.org/10.1016/j.atmosres.2011.10.021

790 Tapas, M., Etheridge, J. R., Howard, G., Lakshmi, V. V., & Tran, T. N. D. (2022). Development of a
791 Socio-Hydrological Model for a Coastal Watershed: Using Stakeholders' Perceptions. AGU Fall

Meeting Abstracts, 2022, H22O--0996.

Tapas, M., Etheridge, R., Miller Julie. Hinckley Brian, H. Z., & Samantha, F. (2022). Hydrological Modeling to Forecast Changes in Eastern North Carolina: Implications for Agriculture, Climate Change, and Fisheries. North Carolina Water Resources Research Institute Annual Conference, 1(Lightning talk)

Thanh, H. V., Binh, D. Van, Kantoush, S. A., Nourani, V., Saber, M., Lee, K. K., & Sumi, T. (2022). Reconstructing Daily Discharge in a Megadelta Using Machine Learning Techniques. Water Resources Research, 58(5). https://doi.org/10.1029/2021WR031048

Tong, K., Su, F., Yang, D., Zhang, L., & Hao, Z. (2014). Tibetan Plateau precipitation as depicted by gauge observations, reanalyses and satellite retrievals. International Journal of Climatology, 34(2), 265–285. https://doi.org/10.1002/joc.3682

Tran, T.-N.-D., Nguyen, Q. B., Zhang, R., Aryal, A., Łukaszewska, M.-G., Sinicyn, G., & Lakshmi, V. (2023a). Quantification of Gridded Precipitation Products for the Streamflow Simulation on the Mekong River Basin Using Rainfall Assessment Framework: A Case Study for the Srepok River Subbasin, Central Highland Vietnam. Remote Sensing, 15(4), 1–27. https://doi.org/10.3390/rs15041030

Tran, T. N. D., Nguyen, Q. B., Vo, N. D., Le, M. H., Nguyen, Q. D., Lakshmi, V., & Bolten, J. (2023b). Quantification of global Digital Elevation Model (DEM) – A case study of the newly released NASADEM for a river basin in Central Vietnam. Journal of Hydrology: Regional Studies, 45(October 2022), 101282. https://doi.org/10.1016/j.ejrh.2022.101282

Wagner, W., Hahn, S., Kidd, R., Melzer, T., Bartalis, Z., Hasenauer, S., Figa-Saldaña, J., De Rosnay, P., Jann, A., Schneider, S., Komma, J., Kubu, G., Brugger, K., Aubrecht, C., Züger, J., Gangkofner, U., Kienberger, S., Brocca, L., Wang, Y., … Rubel, F. (2013). The ASCAT soil moisture product: A review of its specifications, validation results, and emerging applications. Meteorologische Zeitschrift, 22(1), 5–33. https://doi.org/10.1127/0941-2948/2013/0399

Wu, Z., Xu, Z., Wang, F., He, H., Zhou, J., Wu, X., & Liu, Z. (2018). Hydrologic evaluation of Multi-Source satellite precipitation products for the Upper Huaihe River Basin, China. Remote Sensing, 10(6). https://doi.org/10.3390/rs10060840

Xu, Z., Wu, Z., He, H., Wu, X., Zhou, J., Zhang, Y., & Guo, X. (2019). Evaluating the accuracy of MSWEP V2.1 and its performance for drought monitoring over mainland China. Atmospheric Research, 226(April), 17–31. https://doi.org/10.1016/j.atmosres.2019.04.008

Yatagai, A., Kamiguchi, K., Arakawa, O., Hamada, A., Yasutomi, N., & Kitoh, A. (2012). Aphrodite constructing a long-term daily gridded precipitation dataset for Asia based on a dense network of rain gauges. Bulletin of the American Meteorological Society, 93(9), 1401–1415. https://doi.org/10.1175/BAMS-D-11-00122.1

Yuan, F., Wang, B., Shi, C., Cui, W., Zhao, C., Liu, Y., Ren, L., Zhang, L., Zhu, Y., Chen, T., Jiang, S., & Yang, X. (2018). Evaluation of hydrological utility of IMERG Final run V05 and TMPA 3B42V7 satellite precipitation products in the Yellow River source region, China. Journal of Hydrology, 567(May), 696–711. https://doi.org/10.1016/j.jhydrol.2018.06.045